

2021-07

EFFECTS OF PRESTRESSING STEEL BARS ON THE BEHAVIOR OF FIBRE-REINFORCED CONCRETE RAILWAY SLEEPERS

Mekuriachew, Nbret

<http://ir.bdu.edu.et/handle/123456789/12594>

Downloaded from DSpace Repository, DSpace Institution's institutional repository



BAHIR DAR INSTITUTE OF TECHNOLOGY
FACULTY OF CIVIL AND WATER RESOURCE
ENGINEERING
SCHOOL OF RESEARCH AND GRADUATE STUDIES

MSc. Thesis

on

***EFFECTS OF PRESTRESSING STEEL BARS ON THE
BEHAVIOR OF FIBRE-REINFORCED CONCRETE
RAILWAY SLEEPERS***

By

Mekuriachew Nbret

July 2021

Bahir Dar, Ethiopia



BAHIR DAR INSTITUTE OF TECHNOLOGY
FACULTY OF CIVIL AND WATER RESOURCE
ENGINEERING
MSC. PROGRAM IN STRUCTURAL ENGINEERING

EFFECTS OF PRESTRESSING STEEL BARS ON THE
BEHAVIOR OF FIBRE-REINFORCED CONCRETE

RAILWAY SLEEPERS

By

Mekuriachew Nbret

A Thesis Submitted as a Partial Fulfillment to the Requirements for the Award of the Degree of Master of Science in Civil Engineering [Structural Engineering]

Principal Advisor: Tesfaye Alemu (Ph.D.)

Co-advisor: Alemayehu Golla (MSc.)

July 2021

Bahir Dar, Ethiopia

DECLARATION

I certify that the thesis is entitled "*Effect of Prestressing Steel Bars on the Behaviour of Fiber-Reinforced Concrete Railway Sleepers*". It is submitted for partial fulfilment of the degree of Master of Science in Structural Engineering under Faculty of Civil and Water Resource Engineering, Bahir Dar Institute of Technology, a record of original work carried out by me. It has never been submitted to this or any other institution to get any other degree or certificate. The assistance and help I received during this investigation have been duly acknowledged.

Mekuriachew Nbret

Name of the candidate



signature

09/06/2021G.C.

Date

APPROVAL PAGE

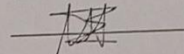
**BAHIR DAR UNIVERSITY
BAHIR DAR INSTITUTE OF TECHNOLOGY
SCHOOL OF RESEARCH AND GRADUATE STUDIES
FACULTY OF CIVIL AND WATER RESOURCE ENGINEERING**

Approval of Thesis for defence

I now certify that I have supervised, read, and evaluated this thesis titled "*Effect of Prestressing Steel Bars on the Behaviour of FRC Railway Sleepers*". Mr Mekuriachew Nbret prepares it under my guidance. I recommend the thesis be submitted for oral defence.

Tesfaye Alemu (PhD)

Advisor's name

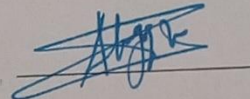

Signature

14/06/2021

Date

Alemayehu Golla (MSc.)

Co-advisor's name


Signature

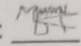
JUL, 29/2021

Date

**BAHIR DAR UNIVERSITY
BAHIR DAR INSTITUTE OF TECHNOLOGY
SCHOOL OF RESEARCH AND GRADUATE STUDIES
[FACULTY OF CIVIL AND WATER RESOURCE ENGINEERING]**

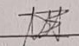
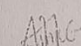
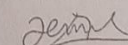
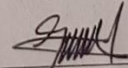
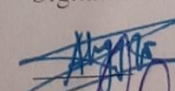
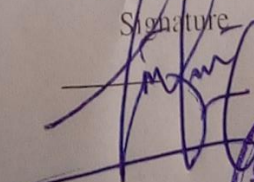
Approval of thesis for defense result

I hereby confirm that the changes required by the examiners have been carried out and incorporated in the final thesis.

Name of Student: Mekuriachew Nbret Signature:  Date: 07/07/2021 G.C.

As members of the board of examiners, we examined this thesis entitled "Effect of Prestressing Steel Bars on the Behaviour of Fiber Reinforced Concrete Railway Sleepers" by Mekuriachew Nbret. We hereby certify that the thesis is accepted for fulfilling the requirements for the award of the degree of Masters of science in "Civil Engineering [Structural Engineering]".

Board of Examiners

Name of Advisor	Signature	Date
<u>Tesfaye Alemu (PhD)</u>	<u></u>	<u>09/07/2021</u>
Name of External examiner	Signature	Date
<u>Abraham Gebre (Dr.)</u>	<u></u>	<u>July 14, 2021</u>
Name of Internal Examiner	Signature	Date
<u>Dr. Temesgen W.</u>	<u></u>	<u>16/07/21</u>
Name of Chairperson	Signature	Date
<u>Temesgan Wolde</u>	<u></u>	<u>JULY 29/2021</u>
Name of Chair Holder	Signature	Date
<u>Alemulu b.</u>	<u></u>	<u>JULY 29/2021</u>
Name of Faculty Dean	Signature	Date
<u>Temesgen Enku Nigussie (PhD)</u> Faculty Dean	<u></u>	<u>JULY 29, 2021</u>



ABSTRACT

Railway sleepers are vital components of a rail network infrastructure. They can be manufactured using different engineered materials. Also, using prestressing steel bars to improve capacity in railway sleepers is an emerging trend in railway engineering. This research numerically investigates the use of embedded prestressed steel bars in steel fibre reinforced railway sleepers. The experimental result reported in the literature was used for validation analysis using ANSYS nonlinear finite element analysis software program. And further, the effects of influential variables such as intensity of prestressing forces, the position of steel bars, grades of concrete, size, and the number of bars to get insight into the behaviour of prestressing steel bars in fibre-reinforced prestressed concrete railway sleepers are studied.

Finite element analysis (FEA) results indicated an increase in grade of concrete improved Load carrying capacity of sleepers on average 17.75 % for each 10 MPa rise in the grade of concrete. Varying prestressing forces did not show a considerable effect on concrete damage and deflection at failure load. In contrast, changing the number and size of tendons exhibited observable effects on the load-displacement response, maximum stress intensity, deformed shape, and plastic strain. Also, positioning steel bars at the bottom rather than at the top and middle of a sleeper resulted in performance gains for railway sleepers.

Keywords: Nonlinear finite element analysis; concrete; sleeper; prestressed; ANSYS

ACKNOWLEDGMENT

First of all, I express my genuine appreciation, respect, and deep gratitude to my Advisor, Dr Tesfaye Alemu, for his invaluable guidance and support throughout this research. This work would not have been possible without his guidance, thoughts, and overall support. Secondly, I would also like to show gratitude to my co-advisor, Mr Alemayehu Golla (MSc.), who helped me through the difficult times and for all of his continuous encouragement.

Afterwards, I would like to thank Mr Belete Molla (MSc.) for his kind help, encouragement, and constructive ideas during this research. I would also like to recognize my helpers at Debre Tabor University and elsewhere to support and inspire.

Lastly, I would like to admit my family for their unconditional love, constant help, prayers, and marvellous support.

Table of Contents

DECLARATION	ii
APPROVAL PAGE	iii
ABSTRACT	iv
ACKNOWLEDGMENT	vi
LIST OF TABLES	x
LIST OF FIGURES	xi
SYMBOLS AND ABBREVIATIONS	xii
CHAPTER ONE	1
1 INTRODUCTION	1
1.1 Background	1
1.2 Statement of the Problem	2
1.3 The objective of the study	2
1.3.1 General objective	2
1.3.2 Specific objectives	2
1.4 Significance of the Study	2
1.5 Scope and Limitations of the Study	3
CHAPTER TWO	4
2 LITERATURE REVIEW	4
2.1 General	4
2.2 Review on Materials for Railway Sleepers	4
2.2.1 Concrete Sleepers	4
2.2.2 Reinforced Concrete Sleepers	5
2.2.3 Prestressed Concrete Sleepers	5
2.2.4 Fibre Reinforced Concrete Sleepers	6
2.3 Review on Prestressing Tendons in Railway sleepers	6
2.4 Review on Loads or Forces on Railway Sleepers	7
2.4.1 Major External Forces on Sleepers	8
2.4.2 Limit States of Railway Sleeper	9
2.5 Review on Major Failures in Railway Sleepers	9
2.5.1 Rail Seat Deterioration	9
2.5.2 Centre-bound damage and longitudinal cracks	10
2.5.3 Impact Loading and Derailment Failures	10
2.6 Review on the Behavior of Railway Sleepers	11
2.6.1 Damping and Energy Absorption	11
2.6.2 Bending moments	11

2.6.3	Stress-Strain Measurements and Strain Rates.....	11
2.6.4	Fatigue and Durability of Railway Sleepers	12
2.6.5	Micro and Macro Cracks of Railway Sleepers	12
2.7	<i>Review of Code of Provisions (EBCS EN 1992-1-1:2013)</i>	13
2.8	<i>Summary of Literature Review and Research Gaps</i>	15
CHAPTER THREE		16
3 METHODOLOGY		16
3.1	<i>Introduction</i>	16
3.2	<i>Validated Experimental Details</i>	16
3.2.1	Geometry details	16
3.2.2	Boundary Conditions and Loading Protocol.....	17
3.2.3	Material Properties.....	18
3.3	<i>Finite Element Analysis Procedures</i>	19
3.3.1	Geometry.....	19
3.3.2	Element Type for Concrete	20
3.3.3	Element Type for Rebar Steel.....	21
3.3.4	Material Type for Concrete.....	21
3.3.5	Material Type for Rebar Steel.....	23
3.3.6	Loading and Boundary Conditions	26
3.3.7	Mesh Sensitivity Study	26
3.3.8	Prestressing Action	29
3.3.9	Analysis type.....	29
3.4	<i>Proposed Parametric Studies</i>	30
CHAPTER FOUR.....		31
4 RESULTS AND DISCUSSIONS		31
4.1	<i>Introduction</i>	31
4.2	<i>Finite Element Validation Analysis Results</i>	31
4.2.1	Load-Displacement Response.....	31
4.2.2	Failure Patterns	33
4.2.3	Validation With Analytical Formulas	34
4.3	<i>Finite Element Parametric Study of Prestressed Railway Sleeper</i>	35
4.3.1	Effect of Grade of concrete.....	35
4.3.2	Effect of Initial stress of tendons	39
4.3.3	Effect of the diameter of prestressing bars.....	42
4.3.4	Effect of number of prestressing bars	44
4.3.5	Effect of position of prestressing bars.....	46

4.3.6	Summary of results	48
CHAPTER FIVE		49
5	CONCLUSIONS AND RECOMMENDATIONS	49
5.1	Introduction.....	49
5.2	Conclusions	49
5.3	Recommendations and Further studies.....	50
REFERENCES		51
APPENDICES		53

LIST OF TABLES

Table 3. 1 Material properties of the selected experiment for validation analysis	18
Table 3. 2 Element geometry	20
Table 3. 3 CPD micro-plane model with CPT215 material data	23
Table 3. 4 Material properties	25
Table 3. 5 MESH200 Element Options (ANSYS help document)	25
Table 3. 6 DOF Constraints and Forces (ANSYS help document)	26
Table 3. 7 Mesh sensitivity analysis	28
Table 3. 8 Proposed parametric study matrix	30
Table 4. 1 Results of tests on sleepers (Anand R. et al., 2020).....	32
Table 4. 2 Maximum load comparisons of NLFEA with test results	33
Table 4. 3 Comparison on load capacity due to effect of concrete grade	36
Table 4. 4 Effect of the grade of concrete on stress intensity and deformation.....	37
Table 4. 5 Comparison on load capacity due to effect of initial stress of tendons	39
Table 4. 6 Effect of initial stress of tendons on stress intensity and deformation	40
Table 4. 7 Comparison on load capacity due to effect of diameter of bars	42
Table 4. 8 Effect of bar diameter on maximum stress intensity and deformation.....	43
Table 4. 9 Comparison on load capacity due to effect of the number of bars	44
Table 4. 10 Effect of number of bars on maximum stress intensity and deformation.	44
Figure 4. 11 Stress intensity and deformation graph for C-60 and Φ 4 sleeper	45
Table 4. 14 Summary of results	48

LIST OF FIGURES

Figure 2. 1 Spacing for pre-tensioned tendons (EBCS EN 1992)	15
Figure 3. 1 One-third scaled sleeper model (Anand . et al., 2020)	17
Figure 3. 2 Schematic diagram for rail seat static test of sleepers	17
Figure 3. 3 Test setup for rail seat static test (Anand . et al., 2020)	18
Figure 3. 4 CPT215 Structural solid geometry (ANSYS help document).....	21
Figure 3. 5 REINF264 Coordinate system and geometry (ANSYS help document) ..	21
Figure 3. 6 Discrete-Reinforcing Modeling Option (ANSYS help document)	24
Figure 3. 7 Discrete-Reinforcing Element Display (ANSYS help document)	25
Figure 3. 8 Free and Mapped Meshes (ANSYS help document)	27
Figure 3. 9 Graph of validation sleeper for mesh sensitivity analysis	28
Figure 4. 1 Force-displacement response of the validation specimen	32
Figure 4. 2 Damage pattern on sleeper subjected to rail seat static test	33
Figure 4. 3 Damage pattern of the validation specimen	34
Figure 4. 4 Ansys result of load-displacement chart for different grades of concrete.	36
Figure 4. 5 Stress intensity and deformed shape graph for 2 Φ 5.6 steel	37
Figure 4. 6 plastic strain graph for 4 Φ 4 steel and 1200 MPa initial stress	38
Figure 4. 7 load-displacement graph for different initial stresses.....	39
Figure 4. 8 Stress intensity and deformed shape graph for sleepers of C-50, Φ 2.8	41
Figure 4. 9 plastic strain graph for sleepers with C-50 and Φ 4 steel.....	42
Figure 4. 10 Stress intensity and deformation graph for C-60 and 800MPa sleeper ..	43
Figure 4. 11 Stress intensity and deformation graph for C-60, 800 MPa and Φ 4 sleeper	45
Figure 4. 12 Maximum plastic strain graph for C-40 and 1200 MPa sleeper.....	46
Figure 4. 13 Stress intensity and deformation graph for C-60, 800 MPa and 2 Φ 5.6 sleeper ..	48

SYMBOLS AND ABBREVIATIONS

RCS	Reinforced concrete sleeper
PCS	Prestressed concrete sleeper
FEA	Finite element analysis
E	Modulus of elasticity
f_c	Uniaxial compressive stress of normal concrete
CDP	Concrete damage plasticity
SFRC	Steel fibre reinforced concrete
NLFEA	Nonlinear finite element analysis
DOF	Degree of freedom
APDL	ANSYS parametric design language
CWR	Continuous welded rail
ANSYS	Analysis system

CHAPTER ONE

1 INTRODUCTION

1.1 Background

The railway infrastructure involves structural elements of ballast, sleeper, rail, and others. Railway sleepers that form an integral part of a rail network mainly transfer weights from the rail pad to the ballast bed. Prestressed concrete sleepers withstand high magnitude wheel loads with no crack during their 50-year service life. The use of steel fibres in the sleepers leads to an increase in load-carrying capacity, energy absorption ability, and consequently improvements in the service life of the sleepers. Steel fibres also help control macrocrack formation (A. Raj. et al., 2020).

The basic principle of prestressed concrete tendons is to transfer the stresses to the concrete. As per different codes, prestressing steels should have a tensile strength \geq of 980 MPa. Prestressing steel bars embedded in the concrete raise both the quality and the resistance to tension and compression characteristics. It also reduced deflections up to 34% in prestressed concrete sleepers (W. Derkowski. et al., 2014). Generally, it may influence the overall performance of a rail network. However, the effect of those prestressing steel bars on the behaviour of railway sleepers subjected to standard wheel load is not been well studied till now.

Simulation of a numerical model only makes sense if it corresponds to the actual experimental model's verification. Prestressed railway sleepers made of fibre reinforced concrete tested in the laboratory are now analyzed using NLFEA in ANSYS Mechanical APDL 2020 R2 for verification.

This research highlights the results of finite element analysis on the effects of prestressing steel bars on fibre-reinforced concrete railway sleepers' behaviour. A standard static load test is carried out on different 36 models with the various magnitude of prestressing stresses, the position of prestressing steel bars, grades of concrete, initial strains of steel bars, size, and amount of prestressing steel bars. The outcomes obtained will be compared with that of a reference sleeper.

1.2 Statement of the Problem

Prestressed concrete sleepers carry and transfer wheel loads from the rails to the ground. Train operations over wheel or rail forces railway sleepers to be in static loading conditions. Using steel fibres in prestressed railway sleepers enhances the load-bearing ability and toughness characteristics. Although they raise the quality and resistance characteristics of sleepers, the contribution of prestressing steel bars on the overall performance of sleepers is not wholly studied till now. This research presents the results of a numerical study through finite element analysis conducted on the effects of prestressing steel bars on fibre-reinforced railway sleepers' behaviour under static wheel loads. The parameters will be different prestressing stresses, the position of bars, grades of concrete, initial strains in bars, size, and the number of steel bars.

1.3 The objective of the study

1.3.1 General objective

- To investigate the effects of prestressing steel bars on fibre-reinforced concrete railway sleepers' behaviour under static wheel loading.

1.3.2 Specific objectives

- To understand the influence of prestressing steel bars' position on the behaviour of steel fibre reinforced concrete railway sleepers
- To evaluate the effect of variation in the grade of concrete for the static load resistance of fibre-reinforced railway sleepers
- To determine the role of initial stresses in prestressing steel bars to improve the capacity of railway sleepers.
- To determine how the size and number of prestressing bars affect the strength of fibre-reinforced railway sleepers

1.4 Significance of the Study

This research investigates how prestressing steel bars' related parameters on fibre reinforced concrete railway sleepers' response under static wheel loading. The outcomes of this study will become principal for developing an improved railway sleeper, i.e., the best combination of variables under this study. The new sleepers' main advantage is an increase in overall capacity that results in better service life. Besides this, this study's outcome can potentially lead to the design guideline for prestressed fibre reinforced concrete sleepers under low magnitude but high-cycle fatigues.

1.5 Scope and Limitations of the Study

This study is limited to prestressed railway sleepers reinforced with steel fibre and subjected to a constant or standard static wheel load of magnitude 440 KN at each rail set. The railway sleepers under this investigation will have an equal length, depth and width with the reference sleeper (one-third scaled-down model of the Indian railway sleeper). The researcher analyzes 36 fibre-reinforced prestressed concrete railway sleeper models. The factors investigated in this study are three different prestressing stresses, the various position of prestressing steel bars, three different grades of concrete, various initial stresses in prestressing steel bars, three combinations of varying size and number of prestressing steel bars for better performance of sleepers to a static wheel load.

CHAPTER TWO

2 LITERATURE REVIEW

2.1 General

Railways as a means of transportation have played a fundamental role in developing all economies to transport goods and passengers. Moreover, it ensures connectivity to different parts of a country at affordable costs to the ordinary person. Railway sleepers are an important railway component laying between two rail tracks to keep the correct spacing of the gauge. Generally applied perpendicular to the rails, sleepers transfer loads to the track ballast and subgrade, hold the rails erect and keep them spaced to the correct gauge.

Most of the loadings on tracks are wheel loads that affect the railway track components' deterioration and undermine sleepers' load-resistant performance. Common causes of failures for railway sleepers are rail seat abrasion, centre bound cracking, and high-magnitude impact loads during a derailment. Many derailments have imparted severe damage to sleepers and delayed the free operations (J. Sykorova et al., 2012). As a result, many railway sleepers do not last until their expected service life. Researches indicate that using steel fibres improves sleeper bending strength, cracking resistance, and energy absorption capacity. It means that the steel fibres can considerably enhance the sleeper service life. Prestressing steel wires raise both the quality and the resistance of the fibre-reinforced concrete railway sleepers.

2.2 Review on Materials for Railway Sleepers

The materials used in the railway sleepers have evolved over the last century. As a result, many materials have been in use in different parts of the world. This paper discusses some of them.

2.2.1 Concrete Sleepers

Concrete offers many advantages in constructing railway sleepers for about half a century due to its improved mechanical characteristics, low permeability, higher resistance against chemical and automated attacks, and sound economic aspects. Moreover, apart from being corrosion resistant compared to other materials, concrete sleepers show high efficiency in controlling creep (A. Raj et al., 2018).

But, the tensile strength of concrete is relatively much lower. Therefore, steel bars enhance their tensile strength, crack arresting and post cracking ductile behaviour of the fundamental matrix.

2.2.2 Reinforced Concrete Sleepers

Reinforced concrete sleepers are used on a larger scale since they are more durable and can withstand exceedingly high compression force without buckling. As a result, RCSs have a longer service life and require less maintenance. In addition, their greater weight helps them remain in the correct position longer. However, due to the inability of steel bars to respond to the plasticity of the concrete in tension, the bond between concrete and steel bars in RCS was susceptible to repeated loading. As a result, slipping of steel bars would occur, and cracking in the concrete takes place. Therefore, the design approach in such members limits the rapidity of crack formation under repeated loading to prolong the service life of the member (Anand Raj, 2018).

2.2.3 Prestressed Concrete Sleepers

The railways across the world have been facing the challenge of improving their competence. As part of their fight to improve the load-carrying capacity and frequency of trips for trains, the use of high-speed lines has gained widespread acceptance. The use of these high-speed tracks has reasonable use of prestressed concrete sleepers. PCS are concrete beams with prestressing steel wires inside of them. The high-strength prestressing cables are of high quality, and the strength will not change over time. They withstand high magnitude loads with no crack occurrence during their service life. PCS is more durable under repeated static Load; hence they are preferred over RCS. It is the starting point of using prestressed concrete as a preferred sleeper in railway lines worldwide (H.J.Taylor, 1993).

The strength and capacity of concrete sleepers depend primarily on the prestressing force and bonds between steel strands and concrete (Warner et al., 1998). Generally, there are two stages for loss of prestressing: initial loss and time-dependent loss.

- Initial loss of prestress in concrete sleepers (due to elastic shortening, bond, friction, and anchorage set) measured between 20 and 27%.
- Over time, the concrete sleepers experience various traffic loads. As a result, they may incur damages and cracks, resulting in a further time-dependent loss in prestress level (because of concrete shrinkage and creep and steel relaxation).

2.2.4 Fibre Reinforced Concrete Sleepers

Railway sleepers working over the world are facing extraordinary performance challenges. Even the wooden and high-quality prestressed concrete sleepers do not stand up to the modern performance demands. Worldwide studies indicate that prestressed concrete sleepers do not complete their intended service life of five decades in many areas.

Researchers have been pursuing various forms of fibres to improve the properties of ordinary concrete. Among the fibres most sought after is steel fibre. Sadeghi J. et al. (2016) have performed studies to device the efficiency and feasibility of using steel fibres to boost the characteristics of sleepers, such as load-bearing ability and toughness. The study results have pointed out that the application of hybrid fibres in sleepers enhances the tonnage and improves energy absorption, consequently improving the service life of the sleepers.

(Parvez A and Foster S J, 2017) Studied the enhancement in fatigue performance of prestressed concrete sleepers when steel fibres are added to them. They added 0.25% and 0.5% by total volume. They reported that fibre sleepers exhibited a 15% improvement in static capacity than those short of fibres. The surface strain of concrete exhibited reduction due to the deed of fibres. Steel fibres in concrete enhanced the crack resistance of concrete. The study points out that a minimum number of fibres is essential for improved performance.

One of the critical assets of steel fibre reinforced concrete (SFRC) is its excellent crack propagation resistance. As a consequence of this ability to arrest cracks, fibre composites possess increased extensibility and tensile strength, both at first crack and ultimate, particularly under flexural loading. In addition, the fibres can hold the matrix together even after widespread cracking. The net effect of all these is to impart the fibre composite pronounce post-cracking elasticity, which is unheard of in ordinary concrete. The change from brittle to the ductile form of material would substantially increase the fibre composite's energy absorption features and its ability to withstand repeatedly applied, shock, or impact loading (Chanh, 2015).

2.3 Review on Prestressing Tendons in Railway sleepers

Although recent, prestressed steel is a material whose origins date back a long way. The adoption of the prestressing technique was attributed to Paxton, who in 1851 utilized this technique to realize the Crystal Palace, unaware of the remarkable discovery he had made.

Koenen was the first to propose prestressing steel bars. He suggested doing this in 1907, before applying concrete, to avoid the formation of cracks.

There are two types of prestressing systems. First, tension the strands and place the concrete in pre-tensioning systems for mass production. Anchor the cables to a strengthened mould. As the concrete has hardened, the lines are released and maintain their tension by their concrete adherence. In post-tensioning systems, tension the tendons after setting the concrete to use in projects with huge elements. Its main advantage is the ability to post-tension both precast and cast-in-place members.

The basic principle of prestressed concrete tendons is to transfer the prestress to the concrete. However, the transfer mechanism between the pre-tensioned and post-tensioned members is different from each other (Amare, 2017). Therefore, this study focuses only on pre-tensioned.

Prestressed steel consists of wires, bars, or strands. The minor tensile strength of high tensile steel bars referring to different codes is 980 N/mm^2 . A prestressing wire is a single element made of steel. The minimal diameters of the cables are 2.5, 3.0, 4.0, 5.0, 7.0, and 8.0 mm. A prestressing strand is spun together of two, three, or seven wires of 2 to 5 mm in a spiral form. A prestressing tendon is a group of strands or wires. A single steel bar can make a tendon. The diameter of a bar is much greater than that of a wire. Prestressing uses high tensile steel bars manufactured in nominal sizes of 10, 12, 16, 20, 22-, 25-, 28- and 32-mm diameter (Amlan K. S. and Devdas M., 2008).

Seven ply pc wire strand with nominal diameters: 12.7, 15.2, 21.8, and 23.5mm is the most popularly used product in prestressing concrete structures (ASTM A416 and BS5896). 7 wire strands with a diameter of 9.53 and 12.5 mm having 1860 MPa tensile strength for prestressing of concrete products produced according to PrEN 10138.

2.4 Review on Loads or Forces on Railway Sleepers

Forces on the track structure are mechanical (static & dynamic) and thermal (Esveld C., 2001).

- Quasi-static loads induced by self-weight of the vehicle and reaction forces in curves;
- Dynamic loads resulting from track irregularities; and
- Thermal loading due to temperature variations in continuous welded rail (CWR).

2.4.1 Major External Forces on Sleepers

The train transportation causes the whole railway track to be under static and dynamic loads. As a result, railway tracks often suffer from extreme loading conditions. The excessive loading is due to the wheel and rail abnormalities, such as the flat wheels, wheel corrugation, out-of-round wheels, dipped rails, etc. These defects can cause loading of a very high magnitude. Still, the short duration and the occurrence of such loading is of low probability during the design life of the sleeper. These forces are often called dynamic or impact forces. Generally, vertical static and dynamic forces are the primary source of railway track problems because of different speeds and different static axle loads on trains (J. Sykorova, 2012).

All static, quasi-static, and impact loads are essential in designing and analyzing railway track components. Static loading represents the mean weight of rail freight wagons, unchanged over a long period. When there are ideal wheel tread and rail surface conditions, the wheel/rail contact force would be identical to static wheel load. Quasi-static loading slightly changes its magnitude over a long period. It is the sum of the static Load and the effect of vehicle speed, together with track support and geometry (curvature, superelevation, and roughness) (A. M. Remennikov and S. Kaewunruen, 2008).

To design a track, we have to use the maximum axle load. A full axle load is a total weight felt by a given axle (20 - 40 ton/axle). It is further related to the mass of rails, the density of sleepers and fixtures, train speeds, and the amount of ballast (Gebeyehu, 2012). The Railway Group Standards-GC/RT5021 (2009) set out requirements of track geometry that are applicable for speed ≤ 225 km/hr and axle loads < 25.5 tones. The design static wheel load per rail seat for standard railway tracks is 125 kN. The static axle loads, however, vary from 50 kN to 350 kN (Esveld, C. (2001) or even to 392 kN (A.R.Foan, 2011) depending on the train type and function.

Zakeri and Sadeghi (2007) summarize the main steps of analyzing and designing railway sleepers based on AS 1085.14-2003. First, considered the design vertical wheel load by neglecting the influence of dead Load. Second, define the Load transferred to the rails' sleepers as a percentage of the design vertical wheel load, 45% to 60% of the rail load. Third, consider a uniform pressure distribution pattern beneath the sleeper and calculate the bending moment at the rail seat and the sleeper's centre. Then, design the capacity of the sleeper accordingly.

2.4.2 Limit States of Railway Sleeper

Relevant limiting conditions to the design of railway sleeper (S. Kaewunruen et al., 2012) are:

- ✓ Ultimate Limit State: - it corresponds to the maximum load-carrying capacity or maximum applicable strain or deformation. For example, a single one-off event such as a severe wheel flat generates an impulsive load capable of failing a single concrete sleeper. Failure under such an event would fit with failures causing severe cracking at the rail seat or the midspan.
- ✓ Damageability (or Fatigue) Limit State: - it is a time-dependent limit state in which a single concrete sleeper accumulates damage progressively over time. For example, such failure could come from excessive accumulated abrasion or cracking growing gradually more severe under repeated impact forces.
- ✓ Serviceability Limit State: - it concerns the regular use. It defines a condition where sleeper failure begins to impose some restrictions on the operational capacity of the track. The loss of a single sleeper is rarely, if ever, a cause of a speed restriction or a line closure. Failure of a cluster of sleepers leads to operational conditions until rectifying the problem.

In general, the critical detrimental factor for the PCSs relies on the ULS. Because the decompression moment due to prestressing of the sleepers minimizes the fatigue damage, the dimension and topology of the sleepers afford the compliments to SLS.

2.5 Review on Major Failures in Railway Sleepers

Rail seat deterioration, centre-bound damage, longitudinal cracks and derailment, and impact loading are primary causes of prestressed concrete railway sleepers' failure.

2.5.1 Rail Seat Deterioration

In recent prestressed concrete sleepers, rail seat deterioration is the most frequent type of failure encountered. The loss of the rail seat is mainly produced either by freeze-thaw cracking, chemical deterioration, hydraulic pressure cracking, rail seat abrasion, and hydro-abrasive erosion. Among those, rail seat abrasion is the most critical one. The loads transferred from the wheels are to the rail, which moves them to the rail pad. The sleepers then take up these loads. When the wheel load is transferred from the cushion to the sleeper, a shear force acts on the rail pad. If the shear force exceeds the fatigue limit of the concrete, deterioration will be started at the rail set. Greve M. J. et al. (2016) found that adding up of damages triggered by crushing in the face of high monotonous loads initiate rail seat deterioration.

2.5.2 Centre-bound damage and longitudinal cracks

Sleepers develop tensile fractures while experiencing high magnitude and high-frequency loads acting during the train movement. For example, a tensile fracture may occur on top of a prestressed concrete sleeper. The freezing of water and fine rocks existing in raw plugs will cause longitudinal cracks. Rezaei F. et al. (2012) have reported longitudinal cracks initiating from fastener locations and propagating to mid-span during and even before track operation. The bending cracks at the midspan reduce the flexural stiffness of the sleeper. The leading cause is infrequent but short-duration high magnitude wheel loads. Cracking of sleepers is a crucial behaviour, not only in mechanical and load-carrying capacity but also in durability and fatigue properties. Often, cracks of sleepers develop and present at the midspan due to excessive negative bending. These cracks can cause broken sleepers and are called a centre-bound problem in railway lines.

Sleepers are required to resist bending moments, which are highest at the rail seat and the centre. During initial installation and later maintenance tamping, the ballast is raised below the rail seats, leading to increased initial pressures on the ballast surface at these locations. Over time the sleeper settles, and the pressure distribution becomes more uniform. Because the ballast at either end of the sleeper is less well confined, the sleeper support becomes concentrated in the middle; a condition referred to as centre binding (T. Rampat et al., 2019).

2.5.3 Impact Loading and Derailment Failures

High magnitude wheel loads act for a short time duration over railway sleepers every time the train passes over them. These occasional loads have a dynamic impact effect and can result in cracks. This type of loading is the consequence of flat wheels and dipped rails. These reasons may convey a force of 400kN on one rail seat for a period of fewer than 10 min. Cyclic loadings cause fatigue of concrete sleepers, which results in permanent progressive changes in the structure. These changes can cause crack propagation, reducing structural behaviour's stiffness, leading to fatigue. Sleepers are principally designed to carry wheel loads from the rails to the ground (Remennikov A M and Kaewunruen S., 2014).

Primary causes of derailment failure are existing impermissible defects in track and human resource's fault. Countless lives have been missing due to the derailment of trains. The massive force that comes upon railway sleepers in the event of derailment damages them beyond repair. Track maintenance cost is increased for replacing those damaged sleepers (A. Raj et al., 2018).

2.6 Review on the Behavior of Railway Sleepers

The current design approach for railway PCS is based on allowable stress. In contrast, the structural behaviours or deformations are kept within the elastic range (AS1085.14-2003).

2.6.1 Damping and Energy Absorption

The capability of tracks to attenuate the vibration and noise depends on the damping ratio of its components. The damping properties of concrete sleepers vary depending on the boundary conditions to which they are subjected. Rail pads, sleepers, and ballast beds play an extreme role in the track's energy dissipation behaviour. The concrete sleepers dissipate the imparted energy by vibration, deformation, and fracture. (Kaewunruen, 2011) have indicated that the concrete sleeper would absorb around 45% of the impact energy as bending curvature and fracture. The remaining portion would accelerate the cracks in sleepers, break the ballast gravel, degrade the rail pad and damage the wheel.

2.6.2 Bending moments

The structural design of concrete sleepers is based on limiting the maximum quasi-static bending moments to proper amounts. The design wheel load, also known as dynamic support-point force, is the force that acts on the sleeper and that produces the design moment. In bending tests, the concrete sleeper must withstand this design moment without the formation of cracks (S. Kaewunruen and A. M. Remennik, 2015. Johansson et al. (2008) showed acceleration and deflection decrease with increasing stiffness of under sleeper pad, an elastic layer used to reduce ballast damage and ground vibration. Steel fibres have been shown to raise the ultimate moment and ultimate deflection of reinforced concrete; the higher the tensile stress because of the fibres, the higher the maximum moment (N. V. Chanh, 2005).

2.6.3 Stress-Strain Measurements and Strain Rates

Loads introduce stress waves in the sleeper. The acceleration of sleepers introduces inertial forces, and the high strain rate changes the material properties of concrete. The concrete behaves in a more brittle manner. As the loading rate increases, its strength, toughness, and modulus of elasticity are also increased. In complex track conditions, the sleeper's vibration results in minor negative strains in the positive zone. Also, cracks could appear in the hard track more rapidly than in a soft way, and this causes the stresses to fluctuate in the lower range.

Strain rate is one of the essential factors that affect the behaviour and performance of sleepers. The mechanical response of concrete members is dependent on the strain rate. By increasing the strain rate for impact and blast loads, the strength of concrete is increased dramatically in both tension and compression (Ngo et al., 2013).

2.6.4 Fatigue and Durability of Railway Sleepers

Fatigue damage of concrete is a significant issue in structural elements subjected to cyclic loading. The railway sleeper is subjected to cyclic loading, which causes fatigue of concrete. When analyzing the fatigue behaviour of concrete, an essential characteristic is the decrease of stiffness, which is calculated using the fatigue damage function (Sýkorová et al., 2008). Salim et al. (2012) have reported that no significant cracks and no reduction in load-carrying capacity were observed from static tests before and after cyclic loads. Some researchers believed that the fatigue life of concrete sleepers would be infinite. Because due to service loads with low magnitude and high cycle, only compressive stress occurs at the sleeper.

Fatigue damage theory, based on fatigue stress, is unsuitable for railway concrete sleepers subjected to periodic impacts. The failure of a railway sleeper is cumulative damage rather than a one-time extreme event that occurs due to derailment. For PCSs, low-magnitude and high-cycle impact fatigue are insignificant compared to the high magnitude but low cycle impact fatigue [Kaewunruen, 2007].

Parvez A. and Foster S. J. (2017) studied the improvement in fatigue performance of PCSs while steel fibres are added to it. They added 0.25% and 0.5% by total volume. They reported that fibre sleepers exhibited a 15% enhancement in static capacity than those without fibres. The study points out that a minimum number of fibres is essential for improved performance. A fibre fraction of 0.5% affords a prolonged fatigue life for concrete sleepers.

2.6.5 Micro and Macro Cracks of Railway Sleepers

Cracks that appear on the rail seat and mid-span are one of the prime concerns for sleepers. They decrease structural stiffness and make the sleepers susceptible to water and chloride-ion penetration, leading to service life reduction. The occurrence of micro-cracks in concrete sleepers due to service loads is unavoidable. Mohammed et al. (2001) showed that cracks could cause significant corrosion of steel bars in concrete.

The purpose of prestressed force on bars is that the stress applied to the wires allows the material to remain compressed, even under bending, which avoids the opening of tensile cracks. The surface strain of concrete is reduced due to fibres. Steel fibres in concrete upgraded the crack resistance of concrete. The width of cracks was decreased due to the presence of fibres as steel fibres bridged the macrocracks developed (Parvez A. and Foster S. J., 2017).

Stages of load-deflection behaviour of concrete structures:

- The first stage shows the linear behaviour of the uncracked elastic section.
- The next phase allows initiation of concrete cracking and
- The last stage relies on yielding steel reinforcements and the crushing of concrete

The load-displacement relations were linear until cracking was initiated. Then, nonlinear relation was obtained as further cracking occurred. Finally, maximum load capacity was reached as crushing and spalling of the concrete in the upper part of the sleeper appeared. The first crack was a flexure crack initiated at the bottom of the sleeper parallel to the applied Load. As the Load was increased, flexure-shear cracks appeared at each side of the flexure crack.

All cracks initiated at the sleeper base are propagated towards the compressive zone beneath the applied Load. As a result, the bending damage stopped. The two flexure-shear cracks mended and became horizontal as the compressive zone in the top of the sleeper was reached.

Besides micro and macroscopic cracks, other factors that influence the durability of concrete sleepers are Rail Seat Abrasion (RSA) and corrosion (Kernes et al., 2011). RSA is the wear degradation under the rail on the surface of PCS. In addition, the durability of sleepers largely depends on ballast condition since it provides support and water drainage (Lutch et al., 2009).

2.7 Review of Code of Provisions (EBCS EN 1992-1-1:2013)

The basis for design work for prestressed-concrete sleepers in Europe is EN 13230. In the USA, the design of prestressed-concrete sleepers is on (AREMA, 2014). To satisfy AREMA and EN 13230, design a new sleeper. This contemporary sleeper conforms to the requirements for an axle load of 347 kN per AREMA. In work based on EN 13230, increase the permissible axle load up to 440 kN. Tests at the Munich Technical University for these high axle loads resulted in successful passing for axle loads of 440 kN as stipulated by EN 13230. The design load is from the static wheel load Q of the train, which calculates 50% of the axle load.

Determine the quasi-static loads from the static loads and the effects of train speed. Australian Standard (AS1085.14, 2003) defines the vertical design loads intended for prestressed concrete sleeper design. Hence, the design load is the combination of both quasi-static and dynamic loads. It shall not be less than 2.5 times the static wheel load.

Prestressing tendons (wires, bars, and strands) shall have an acceptably low level of susceptibility to stress corrosion. The properties of the prestressing tendons are for the materials as placed in their final position in the structure. For steels complying with this, tensile strength, 0.1% proof stress, and elongation at maximum Load are designated, respectively f_{pk} , $f_{p0,1k}$ and ϵ_{uk} . The 0.1% proof stress ($f_{p0,1k}$) and the tensile strength (f_{pk}) are defined as the characteristic value of the 0.1% proof load and the characteristic maximum Load in axial tension, respectively, divided by the nominal cross-sectional area. The design value for the steel stress, f_{pd} , is taken as $f_{p0,1k}/\gamma_s$. The prestressing tendons shall have adequate flexibility and fatigue strength as specified in EN10138. Welds in wires and bars are not recommended.

Structural analysis is performed based on the nominal cross-section area of the prestressing steel and the characteristic values f_{pk} , $f_{p0,1k}$ and ϵ_{uk} . The modulus of elasticity for wires and bars is between 195 and 210 GPa. At the same time, the modulus of elasticity of strands varies from 185 GPa to 205 GPa. The mean density of prestressing tendons for design may generally be taken as 7850 kg/m³. The standards specified above may be practised within a temperature variety between -40°C and +100°C in the finished structure.

The effects of prestressing may be considered as an action or a resistance caused by pre-strain and pre-curvature. In general, prestressing is introduced in EBCS EN 1990:2013 as part of the loading cases. Its effects should be included in the applied internal moment and axial force. The contribution of tendons to the section's resistance should be limited to their additional strength beyond prestressing. Prestressing may be calculated assuming that the effects of prestressing displace the origin of the stress/strain relationship of the tendons. Brittle failure of the member caused by the inability of prestressing tendons shall be avoided.

The force applied to a tendon, P_{max} (the force at the active end during tensioning) shall not exceed the following value:

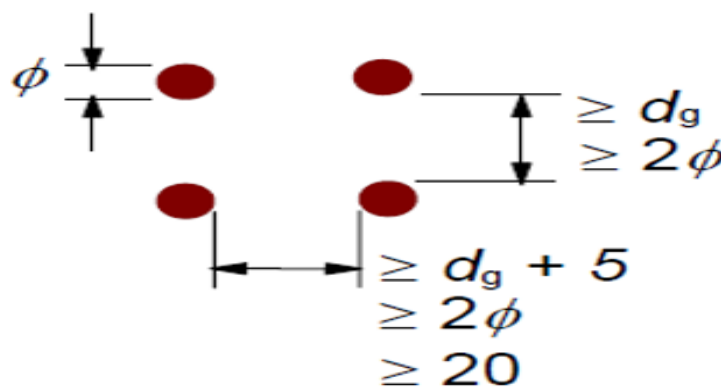
$$P_{max} = A_p * \sigma_{p,max} \quad (eq) 2. 1$$

Where: A_p is the cross-sectional area and $\sigma_{p,max}$ is the ultimate stress applied to the tendon

$$= \min \{ k_1 * f_{pk}; k_2 * f_{p0,1k} \}$$

Note: The recommended values are $k_1 = 0.8$ and $k_2 = 0.9$

The spacing of pre-tensioned tendons shall ensure placing and compacting of the concrete can be carried out satisfactorily. A sufficient bond can be attained between the concrete and the tendons. The minimum precise horizontal and vertical spacing of individual pre-tensioned tendons should be shown in figure 2.1. Consideration should be given to the durability and danger of corrosion of the tendon at the end of elements.



Where Φ is the diameter of pre-tensioned tendon and d_g is the maximum size of aggregate.

Figure 2. 1 Spacing for pre-tensioned tendons (EBCS EN 1992)

2.8 Summary of Literature Review and Research Gaps

Several researchers have studied prestressed concrete railway sleepers over the years to improve their behaviour under static and dynamic loading. Such as upgrading the crack resistance through fibre-reinforcing, strengthening the sleepers with FRP sheets, enhancing the load resistance by increasing the grade of concrete, adding crumbs rubber, etc. Common causes of failures for railway sleepers are rail seat abrasion, centre bound cracking, and high-magnitude impact loads during a derailment. The suggestions over the years have been about using fibre reinforcements that are mainly limited to the concrete part. The variation of parameters related to prestressing steel bars predicting the steel fibre reinforced concrete railway sleeper's behaviour has also not been studied by the previous researchers.

In this research, an attempt was made for the effect of prestressing steel bars on steel fibre reinforced concrete railway sleepers' behaviour under standard static loading using nonlinear finite element analysis.

CHAPTER THREE

3 METHODOLOGY

3.1 Introduction

This research has established a finite element model that simulates and predicts prestressed fibre reinforced concrete sleepers' responses. Validations are also made with related experimental work from the selected article. Generally, the following tasks are performed.

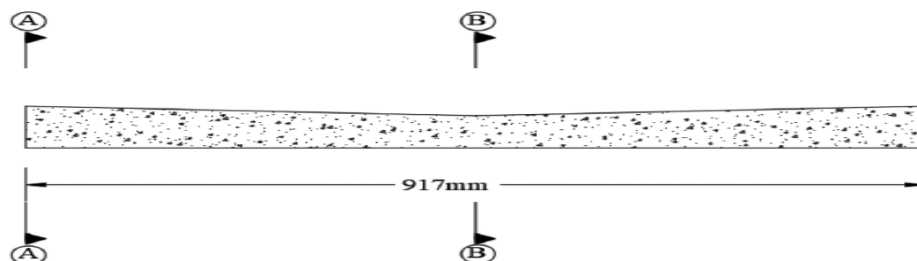
- Related literature is studied, reviewed and the research gap is identified.
- Validation for selected experimental work is done.
- ANSYS is used to model railway sleepers, and static load analysis is carried out.
- Parameters like the different positions of tendons, grades of concrete, initial strains for bars, size, and the number of tendons for railway sleeper models are studied.
- Force-displacement response, crack propagation, stress, and strain for all railway sleepers are analyzed and discussed.

3.2 Validated Experimental Details

Simulation of a numerical model only makes sense if it corresponds to the actual experimental model's verification. Therefore, PCS made of ordinary concrete and fibre reinforced concrete tested experimentally are now modelled using NLFEA in ANSYS Mechanical APDL 2020 R2 for proof. The validation journal paper will be "Investigations on fibre-reinforced rubcrete for railway sleepers" by A. Raj et al. (2020).

3.2.1 Geometry details

A 1/3 scaled-down model of T-2495, an Indian railway sleeper, was used for the study.



a) Elevation of the sleeper model

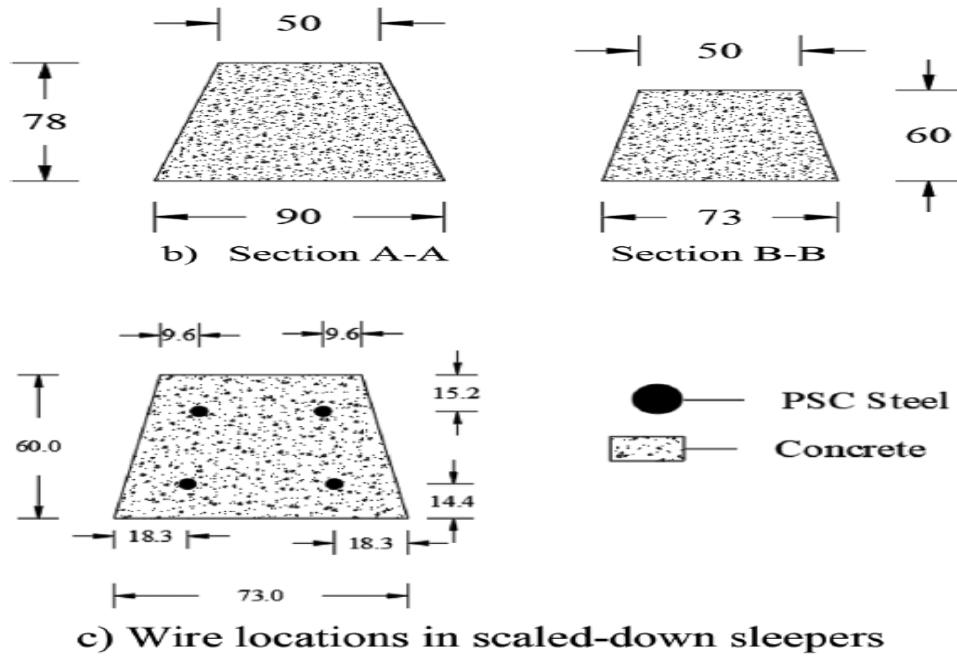


Figure 3. 1 One-third scaled sleeper model (Anand . et al., 2020)

3.2.2 Boundary Conditions and Loading Protocol

Sleeper specimens were exposed to those three assessments based on T-3985 (2011) and composite sleepers' provisional specifications (2017) published by RDSO (Research Design and Standards Organization, Ministry of Indian Railways):

1. Rail seat static test on the two rail seats;
2. Centre top and centre bottom bending tests; and
3. Impact tests.

❖ Rail seat static test on sleepers

The rail seat position is the transmission of the Load from the railway wagon wheels to the sleepers. It is strong enough to convey the weight that is passed on from the wheels. So, rail seat static testing has to be performed to realize the performance of the rail seat. Experimenting was conducted out at one rail seat at a time on a universal testing machine of a capacity of 1000 kN. Throughout testing, the rail seat at the other end was kept unrestrained in the vertical direction.

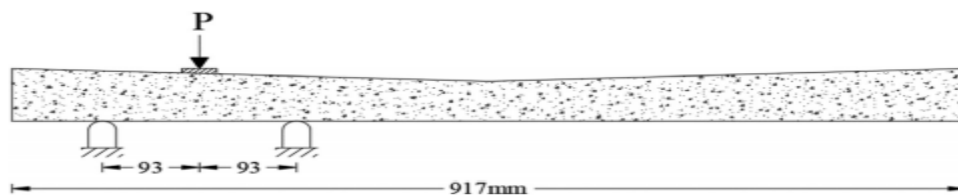


Figure 3. 2 Schematic diagram for rail seat static test of sleepers (Anand . et al., 2020)



Figure 3. 3 Test setup for rail seat static test (Anand . et al., 2020)

3.2.3 Material Properties

Prestressed concrete sleepers were made of 60 MPa cube strength of concrete, and 4 mm diameter high-tensioned steel wires were used for prestressing. Fibres used for the study are 30 mm long and 0.5 mm diameter round crimped steel (0.75 % by volume), having a split tensile strength of 110 MPa. The high-tension cables were first placed through the holes in the mould that was fabricated. Next, the wires were firmly fixed using sockets. Finally, the prestressing force of 10 kN was applied to each of the cables using the prestressing jack. Samples were cast and covered with jute bags for seven days. After seven days, the wires were cut, and the model was de-moulded and kept covered entirely with jute bags and reserved for curing for 28 days.

Table 3. 1 Material properties of selected experiment for validation analysis

Mixture	Comp. strength (N/mm ²)	Split tensile strength (N/mm ²)	Flexural strength (N/mm ²)	Fracture energy (Nm/m ²)
Concrete	69	3.33	5.83	174.64
SFRC	74	3.83	6.35	261.77

For SFRC, $f_{cm} = 74$ MPa, $f_{ck} = f_{cm} - 8 = 66$ MPa and $E_{cm} = 40.1$ GPa, $[4700\sqrt{f_{cm}}$ (ACI)]

Prestressing Steel: No. and size: 4 $\Phi 4$

Modulus of elasticity, $E = 200$ GPa

Initial stress: 795.8 N/mm² $[\sigma = F/A = 10KN / (\frac{\pi 4^2}{4})]$

3.3 Finite Element Analysis Procedures

The substantial part of the sleeper has been modelled using a CPT215 element to predict brittle materials' failure or to predict cracking in tension and crushing in compression. The cracking is determined by the standard of maximum tensile stress, called 'tension cutoff'. The REINF264 element simulates prestressing wires' behaviour to withstand the initial strain attributed to prestressing forces by assuming a perfect bond between these elements and concrete. The pre-tensioning was modelled using initial stress in the tendons corresponding to the prestressing forces at the final stage.

3.3.1 Geometry

The ultimate purpose of FEA is to represent the behaviour of an existing engineering system mathematically. Therefore, the analysis must be an accurate mathematical model of a physical prototype. This model comprises all nodes, elements, material properties, real constants, boundary conditions, and other features used to represent the actual system.

In Mechanical APDL, model generation defines the geometric configuration of the model's nodes and elements. Two different methods can be used to generate a model: solid modelling and direct generation. Solid modelling describes boundaries. It controls the size and desired shape of elements. Finally, it automatically generates all the nodes and elements. With the direct generation method, the location of every node, the size, shape, and connectivity of every aspect is determined before defining these entities.

This research switches between direct and solid models, using different techniques to define parts of the model. Fibre-reinforced prestressed concrete railway sleepers having similar geometries with the validation specimen are modelled and analyzed. The total length of all samples is 925mm, and the top width is 50mm. The centre of the sleeper is 60mm deep and 75mm wide at the bottom. In contrast, the rail seat is 80mm deep and 90mm wide at the base. The prestressing steel bars are positioned at three various locations by varying their position over the height and width of the sleeper.

The points defining the vertices of a model are called key points and are the "lowest-order" solid model entities. In a solid model, key points are created first. Then use those key points to define the "higher-order" solid model entities (that is, lines, areas, and volumes), which are said to be building a model "from the bottom up." The Mechanical APDL program also gives the

ability to assemble a model using geometric primitives, which are fully defined lines, areas, and volumes. As a primitive is created, the program automatically creates all the "lower" entities associated with it. Suppose a modelling effort begins with the "higher" primitive entities. In that case, it is said to be building a model "from the top down." Key points are the vertices, lines are the edges, areas are the faces, and volumes are the object's interior.

A solid model can be "sculpted/shaped" using intersections, subtractions, and other Boolean operations. Booleans allow working directly with higher solid model entities to create complex shapes. (Both bottom-up and top-down creations can be used in Boolean operations.)

According to experimental detail, the control specimen was modelled in ANSYS 2020 R2, a one-third scaled model of an Indian railway sleeper. This approach leads to reducing the computational time and the space of computer disk requirements.

The minimum concrete cover for prestressing tendons shall be 30 mm from the bottom surface and at the ends of the sleeper and 20 mm from the other surfaces EN 13230-6 (2015).

Table 3. 2 Element geometry

	Dimensions (mm)				
	Bottom width		Top Width	Depth	
	@ rail seat	@ the middle		@ rail seat	@ the middle
Group-1	90	75	50	80	60

3.3.2 Element Type for Concrete

CPT215 is a 3-D eight-node coupled solid physics element capable of modelling coupled physics phenomena such as structural-pore-fluid-diffusion-thermal analysis and structural implicit gradient regularization nonlocal field. The feature is described by eight nodes and can have the following degrees of freedom at each node:

- Transformations in the nodal x, y, and z directions
- Pore-pressure (PRES)
- Temperature (TEMP)
- Nonlocal field values (GFV1, GFV2)

CPT215 has elasticity, stress stiffening, large deflection, and extensive strain capabilities.

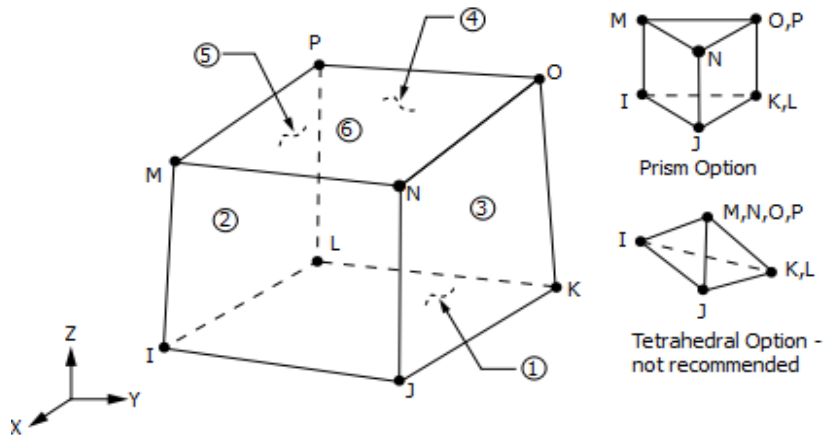


Figure 3. 4 CPT215 Structural solid geometry (ANSYS help document)

3.3.3 Element Type for Rebar Steel

The REINF264 element is suitable for simulating reinforcing fibres with arbitrary orientations. Each thread is modelled separately as a spar that has only uniaxial stiffness or conductivity. Multiple reinforcing fibres can be specified in one REINF264 element. The nodal locations, degrees of freedom, and connectivity of the REINF264 element are identical to those of the base element.

REINF264 has plasticity, stress stiffening, creep, large deflection, and extensive strain capabilities.

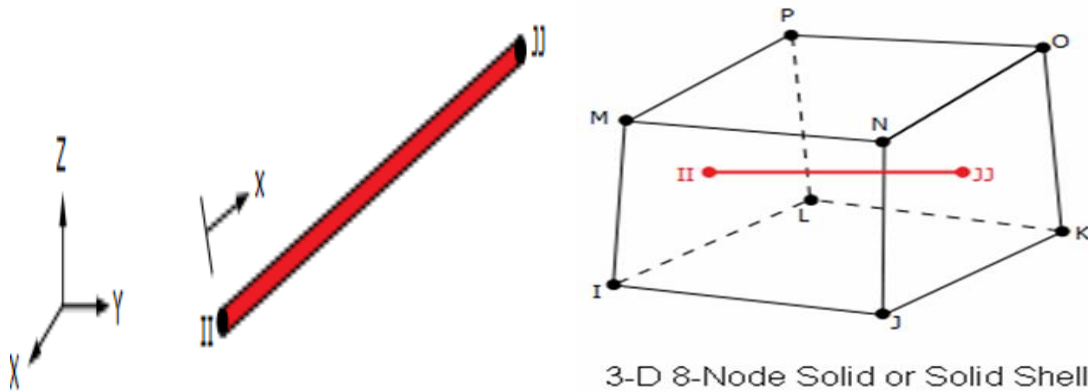


Figure 3. 5 REINF264 Coordinate system and geometry (ANSYS help document)

3.3.4 Material Type for Concrete

In most design codes, including EBCS, the minimum compressive strength of concrete is 40Mpa for pre-tensioned members. For this research, 40, 50, and 60 MPa grades (cylinder strength) of concrete are used as variable parameters.

From EBCS EN 1992-1-1:2013:

$$E_{cm} = 22 \left[\left(\frac{f_{cm}}{10} \right) \right]^{0.3} \quad (Eq) 3. 1$$

$$f_{cm} = f_{ck} + 8 \quad (Eq) 3. 2$$

Where, E_{cm} is the modulus of elasticity of concrete (GPa)

f_{cm} is mean compressive strength of concrete (MPa)

f_{ck} is cylinder compressive strength of concrete (MPa)

The most public value of concrete Poisson's ratio for the design of concrete structures is 0.2.

From previous literature, particularly from the article used for validation, 0.75% steel fibre yields good characteristics to be an optimum percentage to reinforce the prestressed sleeper. Thus, the SFRC has a cylinder compressive strength of 42.9, 53.6, and 66 MPa, respectively.

ANSYS 2020 R2 recommends micro-plane modelling for simulating concrete and engineering materials consisting of various aggregate compositions with differing properties. CPT215 elements in ANSYS 2020 R2 use micro-plane modelling of concrete based on research (Z. P., P.G. Gambarova. 1984) and (Bazant 1985); the material behaviour is modelled through stress-strain laws on several individual planes.

The following micro-plane material model types are available:

- ✓ Elastic damage (non-regularized and regularized forms)
- ✓ Coupled damage-plasticity (regularized form only)

Strain-softening material models often cause mesh sensitivity and numerical instability. It is a problem mitigated by implicit gradient regularization, a class of nonlocal methods. Implicit gradient regularization enhances a local variable by considering its nonlocal counterpart as an extra degree of freedom governed by a Helmholtz-type equation.

The coupled damage-plasticity micro-plane model can be used with the CPT215 coupled pore-pressure-thermal mechanical solid element based on research by Zreid, I. and M. Kaliske (2018). To overcome the numerical instability and mesh sensitivity to which strain-softening materials such as the micro-plane model are susceptible. The model uses an implicit gradient regularization scheme, defined via a nonlocal field, adding two extra degrees of freedom per node.

The plasticity in this model is defined via a three-surface micro-plane Drucker-Prager model, covering a full range of possible stress states and enabling cyclic loading. The damage includes a tension-compression split to account for the transition of the stress state during cyclic loading. In addition, a smooth Drucker-Prager yield function with tension and compression caps cover the material response under all possible triaxialities.

To activate the required extra degrees of freedom (GFV1, GFV2), set KEYO (18) = 2. The additional degrees of freedom require no boundary condition input. A fine mesh is recommended, particularly at probable damage-prone regions. The mesh size may need to be less than half the square root of the nonlocal parameter c .

Table 3. 3 CPD micro-plane model with CPT215 material data (ANSYS help document)

Parameter Type	Parameter Subtype	Parameter (Meaning)	Description (Property)	Constant	Range
Elasticity	-----	E	Modulus of elasticity		
	-----	ν	Poisson's ratio		
Plasticity	Drucker-Prager yield function	f_{uc}	Uniaxial compressive strength	C_1	$f_{uc} \geq f_{ut}$
		f_{bc}	Biaxial compressive strength	C_2	$f_{bc} \geq f_{uc}$
		f_{ut}	Uniaxial tensile strength	C_3	$f_{ut} \geq 0$
	Compression cap	σ_v^c	Intersection point abscissa between compression cap and Drucker-Prager yield function	C_6	$\sigma_v^c \leq -f_{uc}/3$
		R	The major axis over minor axes of the cap	C_7	$R > 0$
	Hardening	D	Hardening material constant	C_5	$D > 0$
R_T		Tension cap hardening constant	C_4	$R_T > 0$	
Damage	-----	γ_{t0}, γ_{c0}	Tension and compression damage thresholds	C_8, C_9	$\gamma_{t0} \geq 0,$ $\gamma_{c0} \geq 0$
	-----	β_t, β_c	Tension and compression damage evolution constants	C_{10}, C_{11}	$\beta_t \geq 0,$ $\beta_c \geq 0$
Nonlocal	-----	c	The nonlocal interaction range parameter		$c \geq 0$
	-----	m	Over-nonlocal averaging parameter		$m \geq 1$

3.3.5 Material Type for Rebar Steel

All the prestressed sleepers are reinforced with three different steel tendons accounting for approximately equal total areas. The number and size of prestressing tendons are 2 $\Phi 5.6$, 4 $\Phi 4$, and 8 $\Phi 2.8$ with different geometry possessing an ultimate tensile strength of 1430, 1715, and 1925MPa. The elastic modulus of prestressing steel was 200GPa, and Poisson's ratio is 0.3.

The cross-section area of reinforcing fibres is small compared to their length. For structural analysis, the bending, torsion, and transverse shear stiffness (all present in beam elements) are ignored in reinforcing elements. Mechanical APDL considers only axial stiffness.

Mechanical APDL assumes a secure mechanical bond between the reinforcing fibres and the base element. The relative movement between these two components is not permitted; therefore, the motion of reinforcing fibres is determined solely by the action of the base element. Based on this simplification, Mechanical APDL adopts the same nodes and connectivity for a reinforcing element and base element.

Mechanical APDL supports two methods for modelling reinforcing cables or fibres:

- ✓ Discrete Reinforcing
- ✓ Smeared Reinforcing

The discrete reinforcing method allows fibres to be accounted for individually. The discrete reinforcing method is suitable for modelling sparsely placed fibres or fibres with inhomogeneous properties, such as cross-section area, material, spacing, and positioning. Discrete reinforcing element, REINF264, combines separate threads to 3-D link, beam, shell, and solid components. The feature supports both structural and thermal analysis. Multiple reinforcing fibres are allowed in a single part.

The smeared reinforcing method is suitable for modelling clusters of reinforcing fibres appearing in layer or sheet form. Each layer of fibres is simplified as a homogeneous membrane having unidirectional stiffness. Fibres in the same layer must have a uniform cross-section, material, spacing, and orientation.

Therefore, the discrete modelling option for reinforcing fibres with nonuniform materials, cross-section areas, or arbitrary orientations is used here. The sections are referenced by REINF264 elements or MESH200 elements when used to define reinforcing locations temporarily.

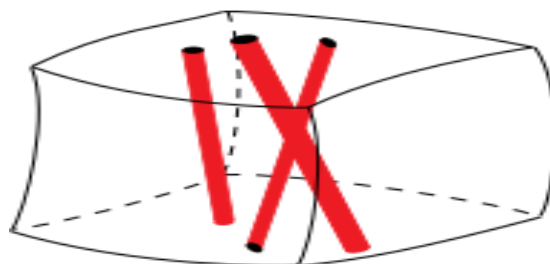


Figure 3. 6 Discrete-Reinforcing Modeling Option (ANSYS help document)

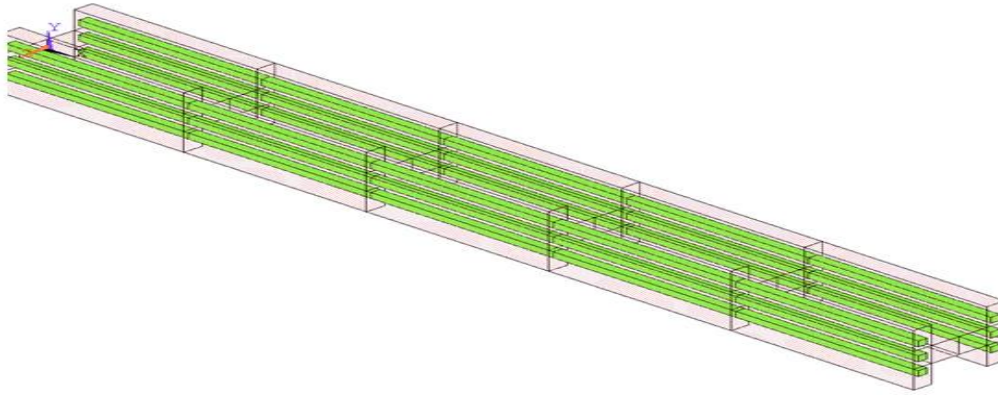


Figure 3. 7 Discrete-Reinforcing Element Display (ANSYS help document)

Creating reinforcing elements is a two-part process:

- ✓ Define the reinforcing material, geometry (such as fibre location, cross-section area, and fibre spacing), and fibre orientation.
- ✓ Generate the reinforcing elements to embed in other structural or thermal (base) elements.

Table 3. 4 Material properties

	SFRC			Prestressing steel		
f_{cm} , (MPa)/Ultimate stress	50.9	61.6	74	1430	1715	1925
Young's modulus (GPa)	35.85	37.96	40.1	200		
Density (kg/m ³)	2400			7850		
Poisson's ratio	0.2			0.3		
Size and number	-----			2Φ5.6, 4Φ4, and 8Φ2.8		

Table 3. 5 MESH200 Element Options (ANSYS help document)

Reinforcing Type	MESH200 Options	Compatible Base Elements
Discrete 3-D	3-D lines with 2 or 3 nodes KEYOPT (1) = 2, 3	Structural Reinforcing: SOLID185, BEAM188,

Generating Reinforcing Elements

A single EREINF command generates reinforcing elements according to the defined reinforcing material, geometry, and fibre orientation. The command determines the reinforcing element type and creates and stores new reinforcements. Reinforcing elements ignore any subsequent modifications made to the base elements. Therefore, ANSYS, Inc. recommends issuing the EREINF command only after the base elements have been finalized.

3.3.6 Loading and Boundary Conditions

The term loads include boundary conditions and externally or internally applied force functions. Loads can be used either on the solid model (on key points, lines, and areas) or the finite element model (on nodes and elements). Loads can be defined directly on the solid model at any time before actually initiating the solution. Thus, solid model loads may be defined before or after finite element meshing. It will automatically be transferred to the finite element model when the solution calculation is begun (when a SOLVE command is issued).

All specimens of railway sleepers under this thesis are subjected to a standard static wheel load of 440 KN. The vertical design wheel load is a maximum static wheel load and service factor, which is assumed 2.5. Thus, a dead load of sleepers is negligible. Dynamic loads may reach high magnitudes depending on the wheels, the rail, or even the support conditions and velocity of the train. Still, the repetition is low (low cycle).

Thus, this research is focused on static Load. A single sleeper bears approximately 50% of the axle load applied directly above it (AREMA, 2014). In reality, the nature of loading situations on railway track structures is somewhat time-dependent. Therefore, significant research attention has been focused on vertical static and dynamic forces. They are the primary source of railway track problems when trains are operated at different speeds and static axle loads.

Table 3. 6 DOF Constraints and Forces (ANSYS help document)

Discipline	Degree of Freedom and Forces	Label
Structural	Translations	U_X, U_Y, U_Z
	Rotations	ROTX, ROTY, ROTZ
	Forces	FX, FY, FZ
	Moments	MX, MY, MZ

3.3.7 Mesh Sensitivity Study

The ultimate objective of building a solid model is to mesh that model with nodes and elements. Once the solid model has been completed, element attributes are set, and meshing controls are established. Then, the Mechanical APDL program can turn free to generate the finite element mesh. A "mapped" mesh containing all quadrilaterals, all triangular, or brick elements can be requested by taking care to meet specific requirements.

The procedure of generating a mesh of nodes and elements consists of three general steps:

- ✓ Set the element attributes.
- ✓ Set mesh controls.
- ✓ Mesh the model

The default mesh controls are appropriate for many models. If no commands are specified, the program will use the default settings (DESIZE) to yield a free mesh. On the other hand, use the intelligent size feature to make a better-quality free mesh. A free mesh has no restrictions regarding element shapes and has no definite shape applied to it. On the other hand, a mapped mesh is limited regarding the component form it comprises and the way of the mesh.

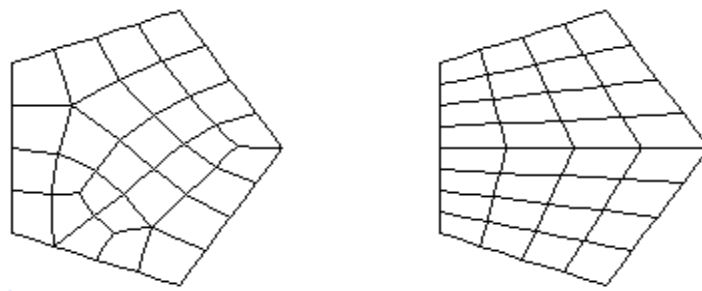


Figure 3. 8 Free and Mapped Meshes (ANSYS help document)

For area meshing, a free mesh can contain only quadrilateral elements, only triangular elements, or a combination of the two. For volume meshing, a free mesh is frequently limited to tetrahedral elements. Pyramid-shaped elements may also be made known into the tetrahedral mesh for transitioning purposes. The mechanical APDL program uses quadrilateral area elements. Triangle area elements or hexahedral (brick) volume elements are also used to generate a mapped mesh. Mapped meshing requires a common area or volume that must meet specific criteria.

The elements used and their mesh size plays a significant role in a numerical simulation. The structural and material properties are programmed within the mesh and determine how the structure will react to certain loading conditions. In finite element modelling, a finer mesh typically results in a more accurate solution. But, as the mesh is made significantly more refined, the computation time increases. Furthermore, the controlled cracking of concrete is one of the most critical aspects of SFRC nonlinear behaviour. One desirable attribute of the finite element method is the convergence of the solution with reasonable mesh refinement. Researchers conducting numerical methods to perform the nonlinear analysis of concrete structural members have noted specific computational difficulties due to mesh dependency influences.

In particular, the element size within an SFRC model has been found to affect the response of structural behaviour, such as the load-displacement characteristics (Shayanfar et al., 1997). The load response behaviour is highly dependent on the cracking propagation and cracks width. To overcome these issues, produce an appropriately sized mesh to efficiently capture the cracking behaviour (Tlemat et al., 2006). Therefore, employing a mesh convergence study consists of refining the mesh size until the numerical behaviour matches the experimental test data. Accordingly, to manage the accuracy and computing resources, a mesh convergence study is performed. The researcher examined load-displacement responses for specimens with 25 mm, 30 mm and 50 mm element sizes to check the mesh sensitivity.

Table 3.7 compares the validation specimen's simulation results using 25mm, 30mm and 50mm element mesh sizes against the test results presented in an experimental study by A. Raj et al. (2020). After conducting the mesh sensitivity analysis, it is found that mesh size 25 mm leads to more reliable results than the other and a good agreement with the test result. Therefore, all the concrete CPT215 elements have meshed with 25mm size tetrahedral elements. The meshing of the rebar element made the exact size of 25mm as steel rebar is a joined element between the spacing of the nodes created by the meshing of the concrete.

Table 3. 7 Maximum load comparison of validation sleeper for mesh sensitivity analysis

	Experiment result	Mesh 25mm	Mesh 30mm	Mesh 50mm
Max' load in KN	57	60.73	51.58	48.69
Error	-	6.54%	9.51%	14.58%

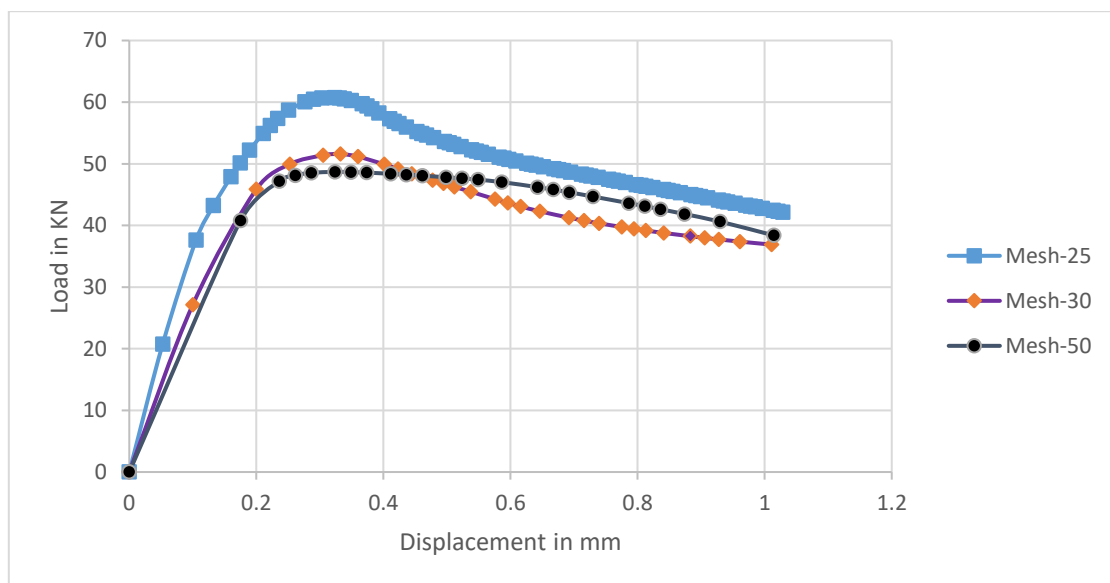


Figure 3. 9 load-displacement graph of validation sleeper for mesh sensitivity analysis

3.3.8 Prestressing Action

The initial state refers to the form of a structure at the start of an analysis. Typically, the assumption is that the initial state is undeformed and unstressed; however, such ideal conditions are not always realistic. The initial-state capability allows defining a nontrivial state from which to start an analysis. The initial state is supported for analysis types (ANTYPE, Antype): Static (Antype = STATIC). After generating reinforcing elements (EREINF), an initial state can be applied directly to each element (INISTATE). For example, an initial state can be used for the MESH200 meshing-facet element. Mechanical APDL then transfers the initial state to the newly generated reinforcing elements automatically.

Although initial stress is element-based, the structure of the INISTATE command is element type-independent. For coupled-field elements, CPT215, the initial stresses to be applied, are Biot's effective strains. They are automatically written out when the output stress option is specified (INISTATE, WRITE, , , ,S). Similar stresses can be applied to all selected elements by issuing an INISTATE, DEFI, ALL command. The INISTATE command can also delete stress from individual components after the stress is applied. Finally, the INISTATE, LIST command lists the applied stresses.

In this research, the initial state is used for stresses. There are three different initial stresses applied to tendons used as a parameter. These are 500MPa, 800MPa, and 1200MPa.

3.3.9 Analysis type

In this study, nonlinear static structural analysis of prestressed concrete railway sleepers was performed in ANSYS Mechanical APDL 2020 R2. The forces, displacements, stresses, and strains in structures caused by loads that do not induce significant inertia and damping effects are determined. Steady loading and response conditions are assumed; that is, the loads and the structure's response are assumed to vary slowly concerning time. In this nonlinear analysis, the total Load applied to FEM was divided into a series of load increments called load steps. According to the nonlinear finite element simulation, load iterations are performed until the convergence criteria are satisfied at each loading step. After reaching the equilibrium and completion of each loading step, the stiffness matrix of the specimen is adjusted to imitate the nonlinear changes in structural stiffness before proceeding to the next load step. An automatic increment with small-time step size and a large maximum number of increments are used to improve the convergence rate.

3.4 Proposed Parametric Studies

ANSYS is general-purpose FEA software that could model reinforced concrete with a high level of accuracy. For the present Study, ANSYS Mechanical APDL 2020 R2 is being used. Accuracy in modelling element type and size, geometry, material properties, boundary conditions, and loads is necessary for the actual member's close numerical idealization.

This research contains modelling of 36 different railway sleepers via a general-purpose finite element package (ANSYS). Load-displacement response, maximum stress intensity, maximum deformation, and maximum plastic strain are analyzed and discussed for various prestressing stresses, the position of tendons, grades of concrete, initial stresses, size and number of tendons. The specimens (S-1 to S-27) are the same as the geometry of the validation specimen that is thicker at the rail seat and becomes thinner and thinner to the sleeper's centre. The models have three different grades of concrete. C-40 (S-1 to S-9), C-50 (S-10 to S-18), and C-60 (S-19 to S-27). Each concrete class are also subdivided into three different initial stresses: 500MPa (S-1 to S-3), 800MPa (S-4 to S-6), and 1200MPa (S-7 to S-9). And finally, each class of initial stresses is further divided into three various combinations of number and size of tendons: 2 Φ 5.6 (S-1), 4 Φ 4 (S-2), and 8 Φ 2.8 (S-3).

Table 3. 8 Proposed parametric study matrix

	Parameters	Constants	Variables
1	Grade of Concrete	4 Φ 4 and $\sigma_i - 800$	C-40, C-50 and C-60
2	Initial Stress of Steel	4 Φ 4 and C - 60	$\sigma_i - 500$, $\sigma_i - 800$ & $\sigma_i - 1200$
3	Diameter of Bars	C - 60, $\sigma_i - 800$ and 2 bars	Φ 5.6, Φ 4 and Φ 2
4	Number of Tendons	C - 60, $\sigma_i - 800$ and Φ 4	2, 3 and 4 tendons
5	Position of Wires	C - 60, $\sigma_i - 800$ and 2 Φ 5.6	Top, Mid, Top& bot and Bot

CHAPTER FOUR

4 RESULTS AND DISCUSSIONS

4.1 Introduction

This chapter aims to describe the findings for all simulated specimens. Validations of the finite element model are employed in ANSYS Mechanical APDL 2020 R2. The critical variables investigated in this study are identified as different positions of tendons, grades of concrete, initial stresses, size, and the number of tendons for railway sleeper models. This chapter presents the validation of the finite element model, results, and discussions of all simulated specimens.

Thirty-six steel fibre-reinforced concrete railway sleeper specimens are analyzed using ANSYS Mechanical APDL 2020 R2 software. The analysis is based on validation of the experimental program on "Investigations of fibre-reinforced concrete for railway sleepers" by A. Raj et al. (2020). Railway sleepers' structural behaviour is discussed in force-displacement response, stress intensity, deformed shape, and strain properties.

4.2 Finite Element Validation Analysis Results

Finite element studies and their comparison with the experimental test results are critical to idealize the actual behaviour of specimens. It also helps to predict behaviours that cannot be tested. Hence, one sleeper previously tested by A. Raj et al. (2020) is selected to validate the finite element model under static loading. This verification could provide evidence about the applicability of the finite element model to investigate structural behaviour. This study is verified against the current experimental work of railway sleepers in chapter three.

In this section, the nonlinear finite element model is validated against the most recent experimental work for SFRC prestressed railway sleepers. The nonlinear finite element model's accuracy is evaluated by comparing the NLFEA result of this specimen with the practical result in terms of load-displacement response and failure pattern.

4.2.1 Load-Displacement Response

The load-displacement response of a structure indicates the capacity of the system due to applied loads. The optimum percentage of steel fibres, the proportion by volume, was obtained experimentally as 0.75%. Steel fibres switch macrocracks and boost the strength property by

linking different concrete constituents. They rise to a 10% ultimate load for steel fibre reinforced concrete sleepers subjected to rail seat static tests.

The addition of steel fibres resulted in the ultimate Load for SF0.75 sleeper being 11% of 57 kN higher than that of the reference specimen subjected to the first rail seat static test. In addition, a rise of 83% was noticed in energy absorbed for SF0.75 sleepers compared to the controlled sample. Such an increase can be credited to the higher power required to break the bonds created by steel fibres between the developed cracks.

The load-displacement response of the validation specimen obtained by the NLFEA shows good agreement with the experimental result, as displayed in figure 4.1. The average maximum Load obtained from the NLFEA of this specimen is 6.54% higher than the maximum Load reported from the experimental study (refer to Table 4.2).

Table 4. 1 Results of tests on sleepers (Anand R. et al., 2020)

Ultimate loads of rail seat static test	
Specimen ID	Rail seat static test, KN
SF0	51
SF0.75	57

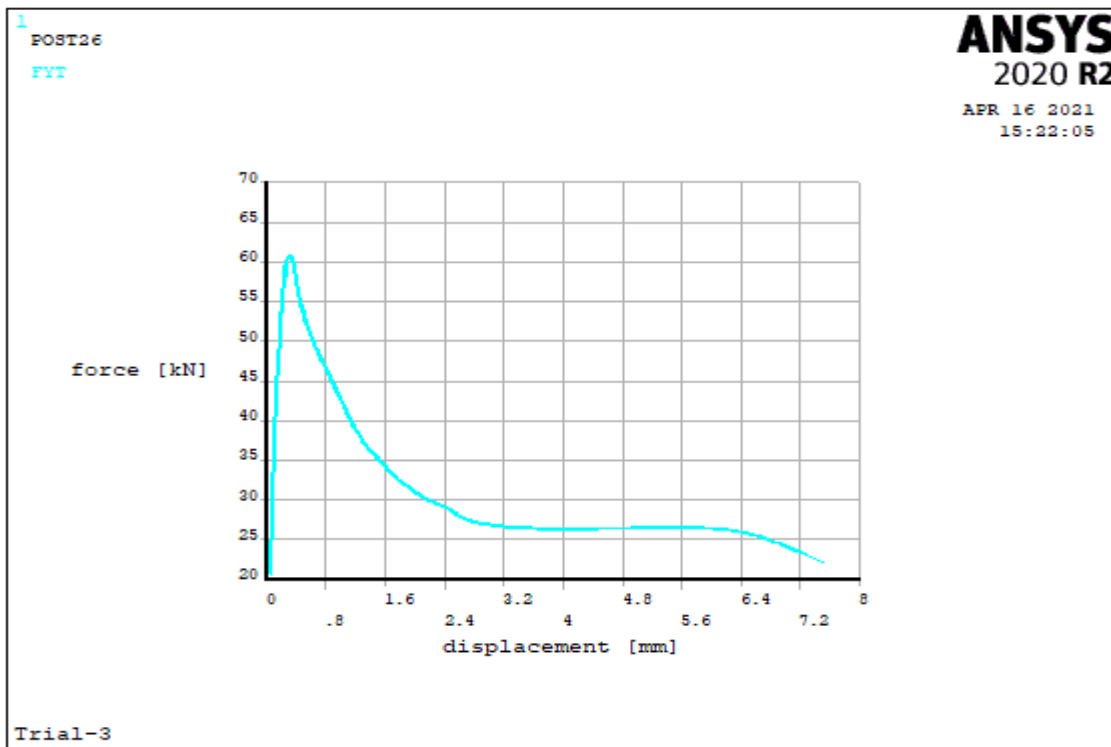


Figure 4. 1 Force-displacement response of the validation specimen

To describe the overall model accuracy of the NLFEA, the error (%) and mean model accuracy [M (%)] evaluated based on the relation given in (Behnam et al., 2018) and is defined as:

$$Error(\%) = \left| \frac{NLFEA\ result - Test\ result}{Test\ result} \right| \times 100$$

$$Mean\ Model\ Accuracy, M(\%) = \frac{NLFEA\ result}{Test\ result} \times 100$$

Table 4. 2 Maximum load comparisons of NLFEA with test results of the specimens.

Specimen	Average maximum Load (kN)		Prediction	
	NLFEA	Test	M (%)	Error (%)
	60.73	57	106.54	6.54

As presented in Table 4.2, the maximum load model prediction leads to an error of about 6.5%, which shows that the specimen's finite element response is in excellent agreement with the results reported from the experimental study.

4.2.2 Failure Patterns

As shown in the following figures, the numerical model shows good agreement between the damage pattern around the supports obtained by NLFEA and the cracking propagation pattern reported in the experimental study. Furthermore, this specimen's projected NLFEA cracking pattern is concentrated on the load application point to test cracks. Therefore, the nonlinear finite element model confirms strong capability in predicting the failure of the specimens. This result also further approves the accuracy of the finite element model.

For steel fibre-reinforced concrete sleepers (SF0.75), the ability of steel fibres to control crack initiation supports the enhancement of maximum loads. When the cracks were created in the material, the steel fibres detained the components in place for a longer time without a quicker deterioration of the concrete bond.



Figure 4. 2 Damage pattern on sleeper subjected to rail seat static test (Anand R. et al. 2020)

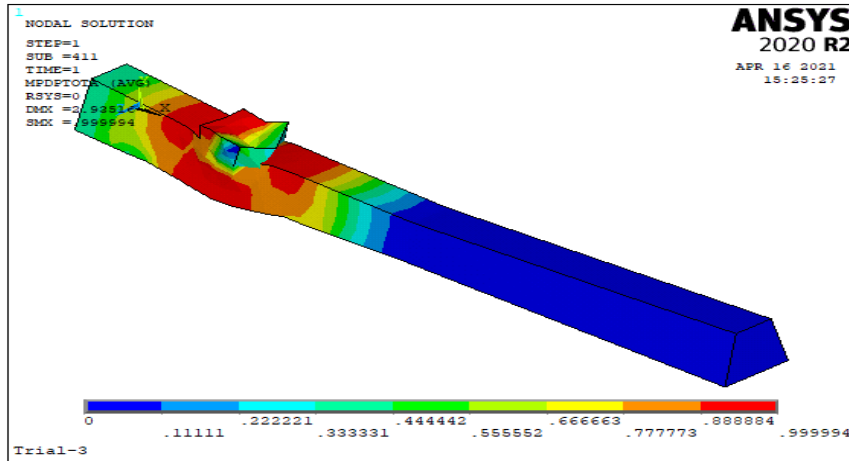


Figure 4. 3 Damage pattern of the validation specimen

4.2.3 Validation With Analytical Formulas

In prestressed single-span members without shear reinforcement, the shear resistance of the regions cracked in bending may be calculated using Expression (EBCS EN 1992-1-1-2013).

$$V_{Rd,c} = [C_{Rd,c} k (100 \rho_1 f_{ck})^{1/3} + k_1 \sigma_{cp}] b_w d$$

Where $V_{Rd,c}$ is the design shear resistance of the member without shear reinforcement in [N].

$$k = 1 + \sqrt{\frac{200}{d}} \leq 2.0 \text{ with } d = 73.8 \text{ mm}$$

$$\rho_1 = \frac{A_{s1}}{b_w d} \leq 0.02$$

A_{s1} is the tensile reinforcement area = 50.27 mm²

$$b_w = \frac{a+b}{2} = \frac{50+85.4}{2} = 67.7 \text{ mm, smallest width of the cross-section in the tensile area}$$

σ_{cp} = Compressive stress of concrete at the centroidal axis due to prestressing = $\frac{P_t}{A_c} = 30.3$

P_t is prestressing force at transfer = $f_{ct} \times A_{net} = 151,405.74$

f_{ct} is allowable stress of concrete under compression = $0.6 \times f_{ck} = 30.6 \text{ MPa}$

f_{ck} is 28 days Characteristic compressive cylinder strength of concrete = $0.85 f_c = 51 \text{ MPa}$

f_c = Compressive strength of concrete, cube/grade = 60 MPa

$$A_{net} = A_c - A_{s1} = 4998.2 - 50.27 = 4947.9 \text{ mm}^2$$

A_c is the concrete cross sectional area [mm²] = 4998.2

$$\rho_1 = \frac{50.27}{67.7 \times 73.8} = 0.011 \leq 0.02$$

$$k = 1 + \sqrt{\frac{200}{73.8}} = 2.65 > 2.0, \text{ take } k = 2$$

$$C_{Rd,c} = \frac{0.18}{\gamma_c} = \frac{0.18}{1.5} = 0.12, \gamma_c = \text{Partial factor for concrete} = 1.5 \text{ at ULS}$$

k_1 is 0.15.

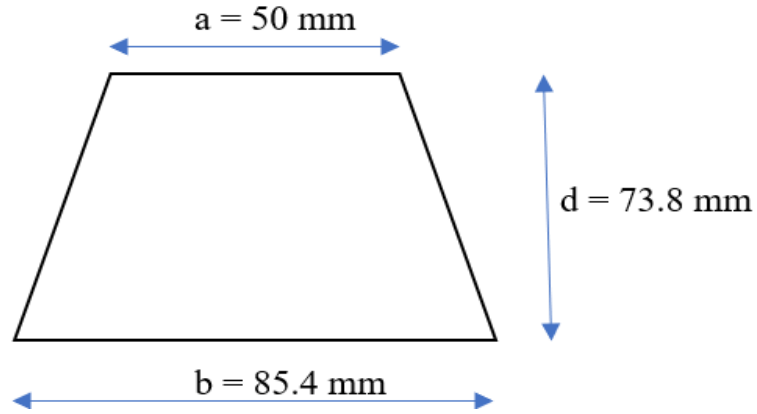


Fig. Sleeper cross-section at the point of load application

$$\text{Then, } V_{Rd,c} = [0.12 \cdot 2 \cdot (100 \cdot 0.011 \cdot 51)^{1/3} + 0.15 \cdot 30.3] \cdot 67.7 \cdot 73.8 = 27.3 \text{ KN}$$

Since the sleeper is supported with two-pin conditions, the design shear resistance of the member without shear reinforcement is the same as one of the reaction forces at the support.

$$V_{Rd,c} = \frac{P_d}{2} \Rightarrow P_d = 2V_{Rd,c} = 54.6 \text{ KN}$$

The analytical load-carrying capacity of the section is about 54.6 KN.

The numerical outputs show a good agreement with the analytical result. The deviation of the numerical work is only about 10% from the analytical results.

4.3 Finite Element Parametric Study of Prestressed Railway Sleeper

This section presents the finite element analysis findings and discussions of all models. It is focused to study the effects of prestressing steel bars on the behaviour of prestressed steel fibre reinforced concrete railway sleepers under static loading.

4.3.1 Effect of Grade of concrete

A parametric investigation is conducted on 27 models to study the effect of the grade of concrete. Railway sleepers with C-40, C-50, and C-60 concrete with three different initial stresses, the position of bars, and three combinations of numbers and diameter of steel bars are used. The analysis results are discussed in the following subsection based on load-displacement responses, stress intensity, maximum deflection, and plastic strain from ANSYS 2020 R2.

I. Effect of the grade of concrete on load-displacement responses

The load-displacement response plots of specimens with 4Φ4 bars and 800MPa initial stress are presented in Figure 4.4. The comparison of their peak loads is shown in Table 4.3.

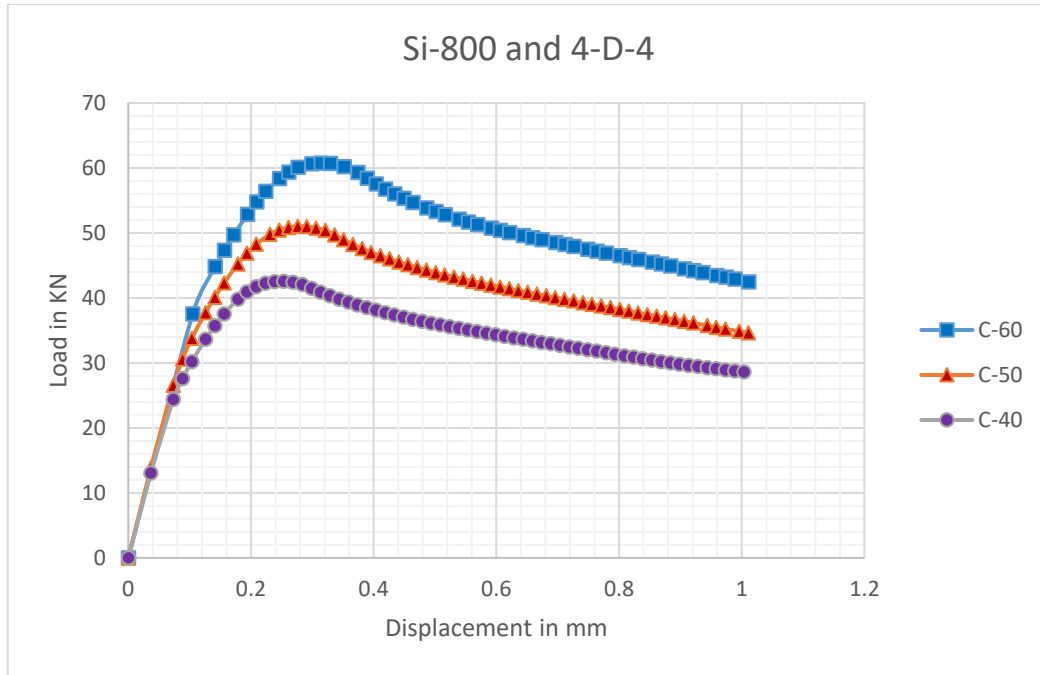


Figure 4. 4 Ansys result of load-displacement chart for different grades of concrete

As shown in Figure 4.4, all load-displacement responses demonstrate a typical stable elastic linear response up to the yield point. A non-linear behaviour for different models followed them. ANSYS result of nonlinear analysis of sleepers with C-40, C-50, and C-60 grade of concrete yields an average load of 42.58KN, 51.04KN, and 60.72KN with corresponding average deflections of 0.25mm, 0.28mm, and 0.31mm at yield load, respectively.

Table 4. 3 Comparison on load capacity due to effect of concrete grade

	2 Φ 5.6		4 Φ 4		8 Φ 2.8		Average	
	Load	Displacement	Load	Displacement	Load	Displacement	KN	Mm
C-60	60.64	0.311	60.75	0.314	60.76	0.314	60.72	0.313
C-50	50.99	0.279	51.04	0.276	51.08	0.279	51.04	0.278
C-40	42.55	0.247	42.58	0.254	42.62	0.247	42.58	0.249

Generally, as the grade of the concrete increases, the maximum load-carrying capacity of the specimen and its deflection at yield load increases.

II. Effect of the grade of concrete on stress intensity and deformed shape responses

From ANSYS Mechanical APDL 2020 R2 non-linear analysis of different grades of concrete on railway sleepers, the average maximum stress intensity becomes 177KN/m², 182KN/m², and 191KN/m² with a corresponding average maximum deflection of 10.51mm, 9.9mm, and 8.22mm for C-40, C-50 and C-60 grades of concrete respectively.

Table 4. 4 Effect of the grade of concrete on maximum stress intensity and deformation

Grade of concrete	Max' displacement, DMX (mm)				Max' Stress Intensity, SMX (KN/m ²)			
	2 Φ 5.6	4 Φ 4	8 Φ 2.8	Average	2 Φ 5.6	4 Φ 4	8 Φ 2.8	Average
C-40	7.76	18.37	5.40	10.51	171	188	171	177
C-50	7.20	17.33	5.17	9.9	182	183	182	182
C-60	6.56	12.56	5.55	8.22	189	192	192	191

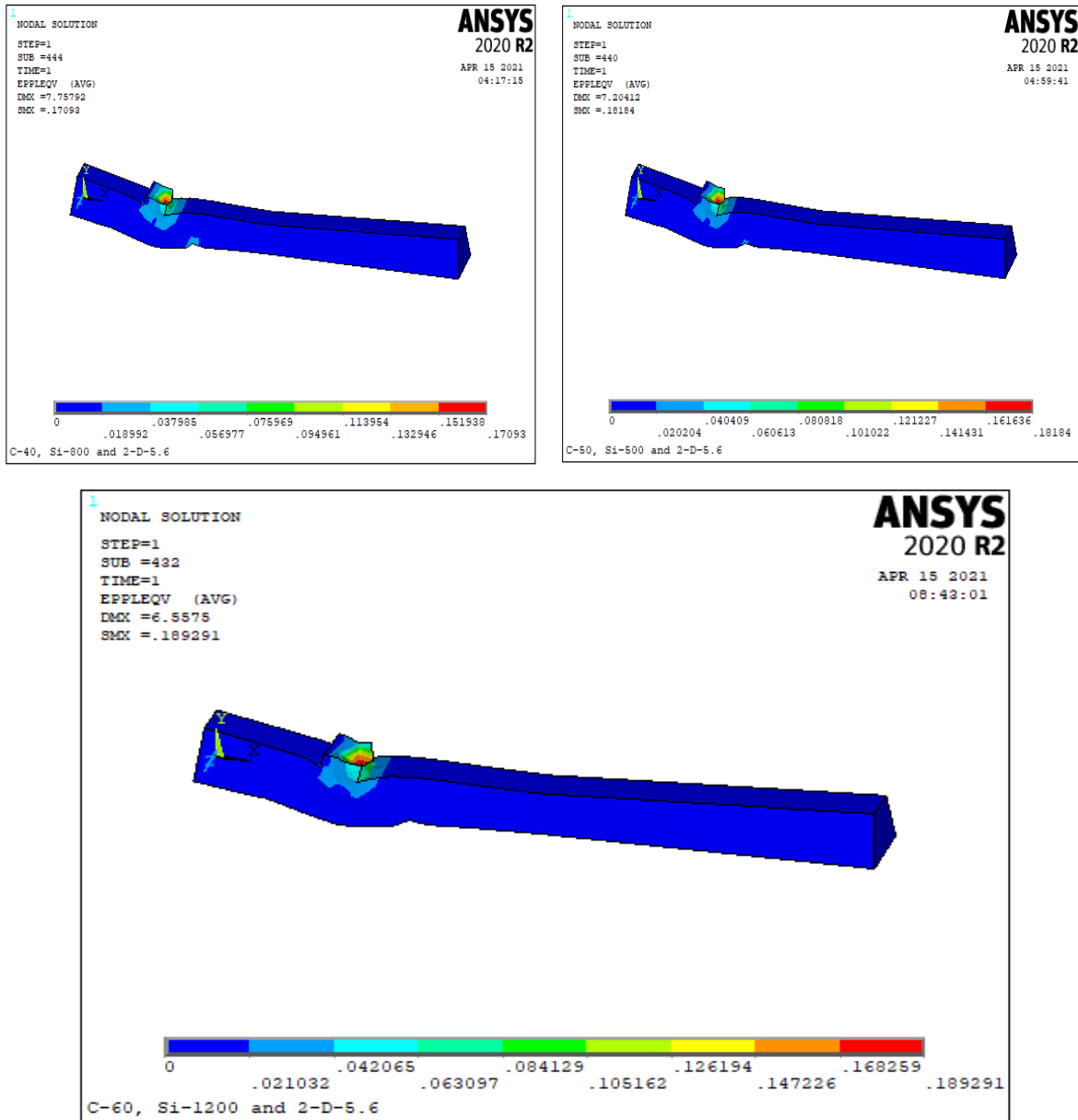


Figure 4. 5 Stress intensity and deformed shape graph for 2Φ5.6 steel

Generally, as the grade of the concrete increases, the maximum stress intensity of the specimen is increased, and its maximum deflection has decreased.

III. Effect of the grade of concrete on plastic strain response

Plastic strain refers to a concrete damage plot. It is permanent deformation and does not return to its original size and shape after the deforming force has been removed. For example, the ANSYS 2020 R2 FE nonlinear analysis on C-40, C-50, and C-60 grades of concrete railway sleepers prestressed with $4\Phi 4$ steel bars with 1200 MPa initial stress resulted in a corresponding maximum plastic strain $0.416E-5$, $0.442E-5$ and $0.495E-5$.

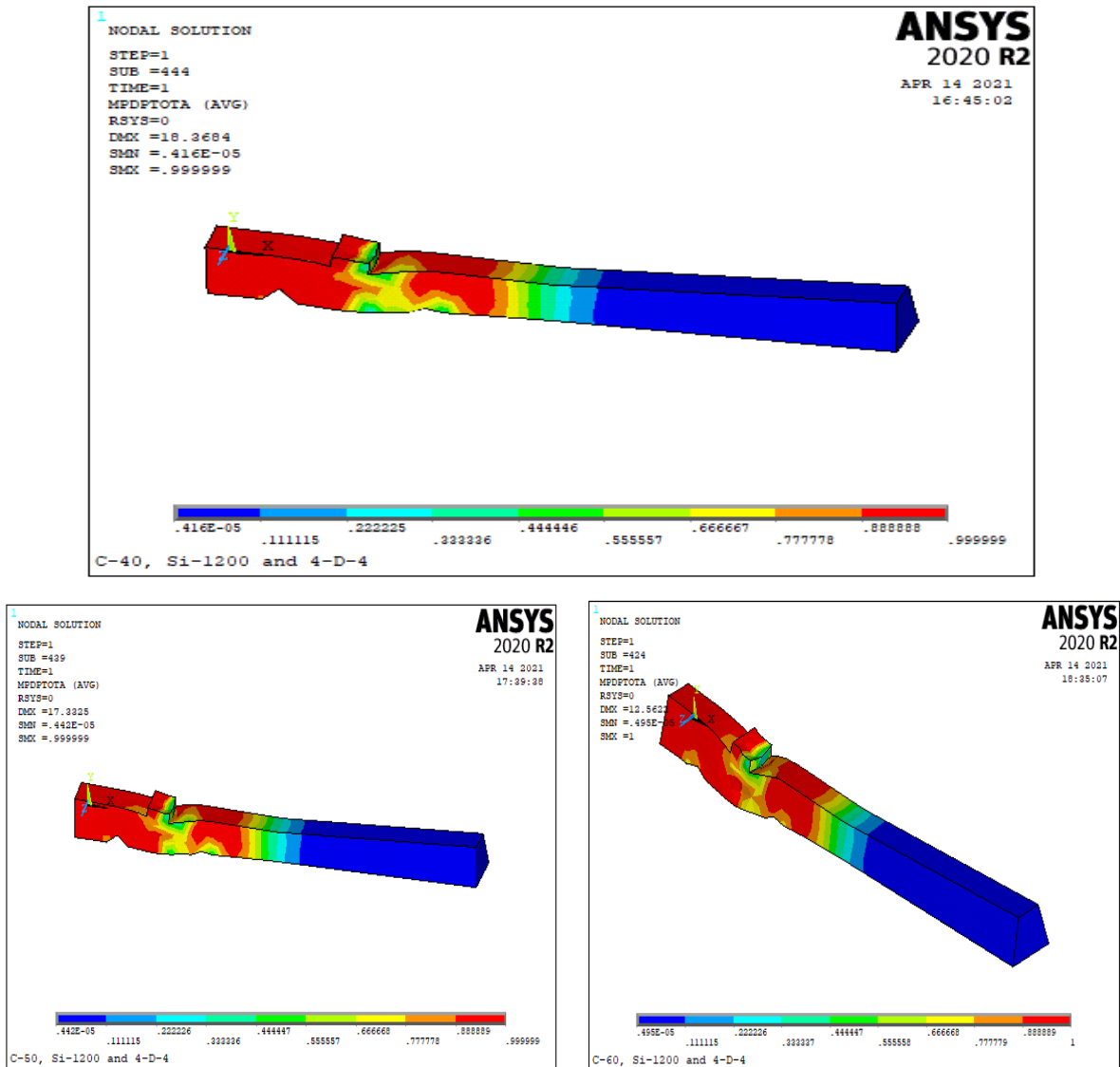


Figure 4. 6 plastic strain graph for $4\Phi 4$ steel and 1200 MPa initial stress

Generally, as the grade of the concrete increases from 40 to 50 and then to 60 MPa, the maximum plastic strain of the specimen shows increment correspondingly.

4.3.2 Effect of Initial stress of tendons

A parametric investigation is conducted on 27 models to study the impact of the initial stress of tendons. Railway sleepers with 500MPa, 800MPa, and 1200MPa stress were initially applied to steel bars with three different concrete grades and combinations of the number and diameter of steel bars are used. The analysis results are discussed in the following subsection based on load-displacement responses, stress intensity, maximum deflection, and plastic strain from ANSYS Mechanical APDL 2020 R2 results.

I. Effect of initial stress of tendons on load-displacement responses

The load-displacement response plots of specimens with C-60 concrete and 4Φ4 prestressing bars are presented in Figure 4.7, and the comparison of their peak loads are shown in Table 4.5

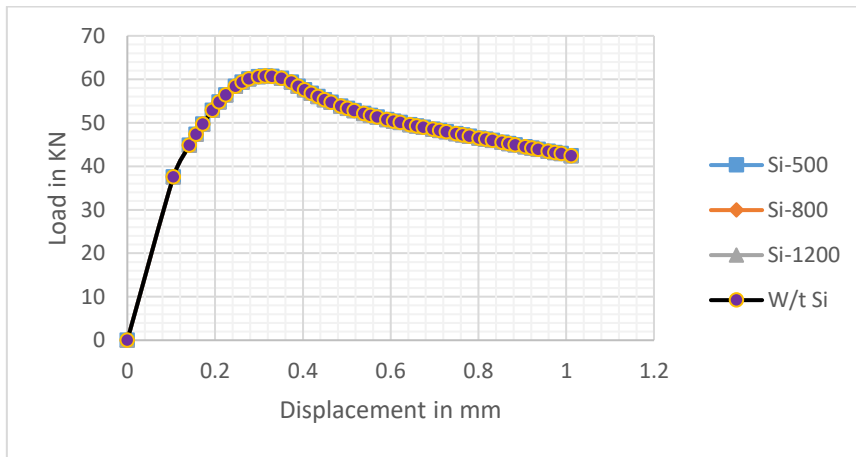


Figure 4. 7 load-displacement graph for different initial stresses

As shown in Figure 4.7, the sample specimens' load-displacement responses demonstrate a typical stable elastic-linear response to the yield point. A non-linear behaviour for different models followed them. ANSYS result of nonlinear analysis of sleepers with 500MPa, 800MPa, and 1200MPa initial stress of bars yields an average load of 60.75KN with corresponding average deflections of 0.314mm at yield load, respectively.

Table 4. 5 Comparison on load capacity due to effect of initial stress of tendons

		2 Φ 5.6		4 Φ 4		8 Φ 2.8	
		Load	Displacement	Load	Displacement	Load	Displacement
$\sigma_i = 500,$	C-40	42.55	0.247	42.58	0.254	42.62	0.247
800 and	C-50	50.99	0.279	50.03	0.276	51.08	0.279
1200	C-60	60.64	0.311	60.75	0.314	60.76	0.314

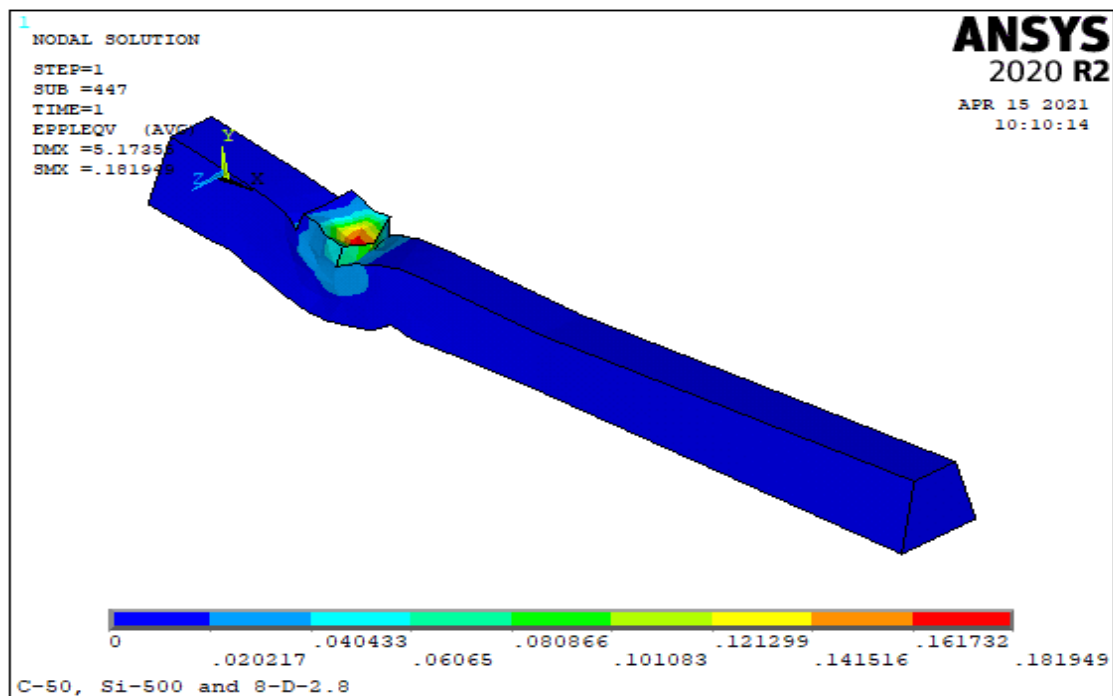
Although the initial stress of steel bars varies, the maximum load-carrying capacity of the specimen and its deflection at yield load do not show any observable change. Therefore, one can conclude that the initial stress of tendons has no considerable effect on the load-displacement response of prestressed concrete railway sleepers.

II. Effect of initial stress of tendons on stress intensity and deformed shape responses

From ANSYS Mechanical APDL 2020 R2 non-linear analysis of different initial stresses of steel bars on railway sleepers with C-50 grade of concrete and 8Φ2.8 steel bars, the average maximum stress intensity becomes 182 KN/m² with a corresponding average maximum deflection of 5.16mm for all 500 MPa, 800 MPa, and 1200 MPa stresses.

Table 4. 6 Effect of initial stress of tendons on maximum stress intensity and deformation

		2 Φ 5.6		4 Φ 4		8 Φ 2.8	
		SMX	DMX	SMX	DMX	SMX	DMX
$\sigma_i = 500,$ 800 and 1200	C-40	171	7.76	188	18.37	171	5.40
	C-50	182	7.20	183	17.33	182	5.16
	C-60	189	6.56	192	12.56	192	15.55



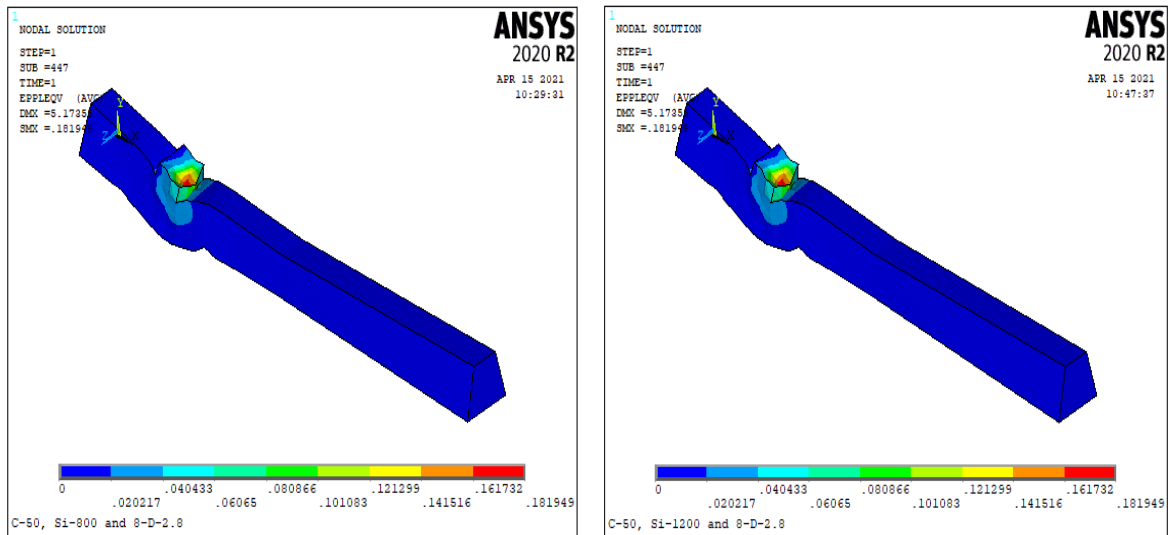
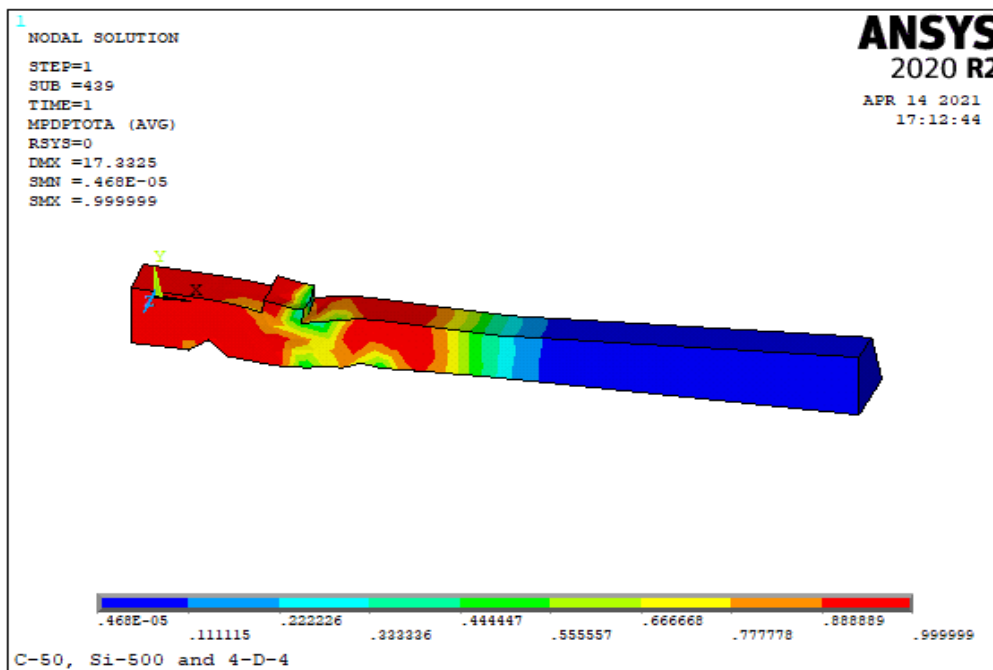


Figure 4. 8 Stress intensity and deformed shape graph for sleepers with C-50 and 8Φ2.8 steel

Generally, as the initial stress of steel bars varies, the maximum stress intensity of the specimen and its maximum deformation do not show any observable change. Therefore, the initial stress of tendons has no considerable effect on the stress intensity and deformed shape response of prestressed concrete railway sleepers.

III. Effect of initial stress of tendons on plastic strain response

The ANSYS 2020 R2 FE nonlinear analysis on 500MPa, 800MPa, and 1200MPa 4Φ4 steel bars initially stressed railway sleepers with C-50 grade of concrete results in a corresponding maximum plastic strain 0.468E-5, 0.468E-5 and 0.442E-5 respectively.



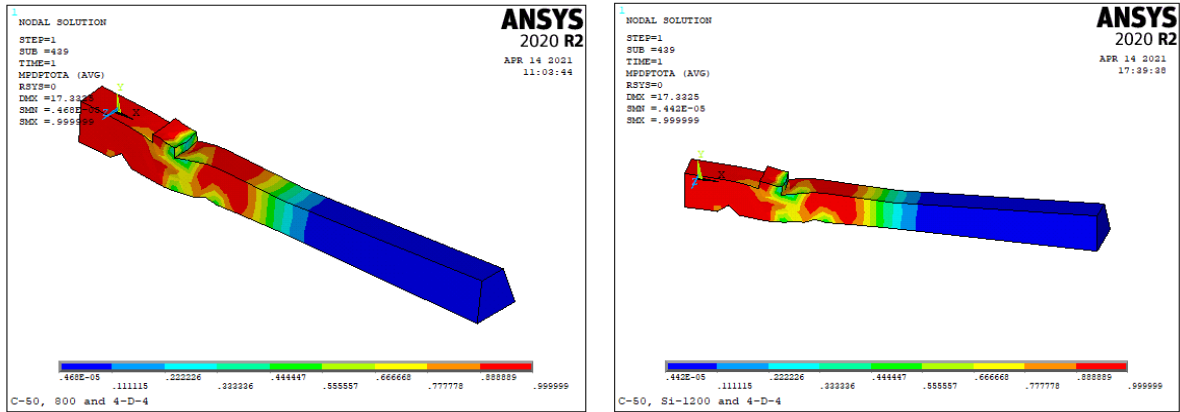


Figure 4. 9 plastic strain graph for sleepers with C-50 and $\Phi 4$ steel

Generally, as the initial stress of steel bars increases from 500 MPa to 800 MPa and then to 1200 MPa, the maximum average plastic strain of the specimen doesn't show any decrement correspondingly for different sizes and numbers of tendons.

4.3.3 Effect of the diameter of prestressing bars

The parametric investigation is conducted on three models to study the diameter of prestressing steel bars. Railway sleepers with 2 Φ 5.6, 2 Φ 4, and 2 Φ 2.8 tendons with C-60 concrete grade and 800MPa initial stress bars are used. The analysis results are discussed in the following subsection based on load-displacement responses, stress intensity, maximum deflection, and plastic strain from ANSYS Mechanical APDL 2020 R2 results.

I. Effect of the diameter of bars on load-displacement responses

The load-displacement response of specimens is presented in the comparative form of their peak loads, as shown in Table 4.7.

Table 4. 7 Comparison on load capacity due to effect of diameter of bars

	Load (peak), N	Displacement @ peak load, mm
2 Φ 5.6	60,637	0.311
2 Φ 4.0	60,611	0.323
2 Φ 2.8	60,600	0.323

As shown in the above table, sleepers with 2 Φ 5.6, 2 Φ 4, and 2 Φ 2.8 prestressing steel bars yields a peak load of 60,637N, 60,611N and 60,600N with corresponding deflections 0.311mm, 0.323mm and 0.323mm at yield load respectively. Generally, make other variables constant; as the diameter of bars decreases, the maximum load-carrying capacity of the specimen is also decreased. Still, the deflection at this load has increased.

II. Effect of the diameter of bars on stress intensity and deformed shape response

From ANSYS non-linear analysis of diameter of steel bars on railway sleepers, the average maximum stress intensity becomes 189KN/m^2 , 184KN/m^2 , and 183KN/m^2 with a corresponding average maximum deflection of 6.56mm , 2.94mm , and 2.94mm for $2\Phi 5.6$, $2\Phi 4$ and $2\Phi 2.8$ prestressing steel bars respectively.

Table 4. 8 Effect of the diameter of bars on maximum stress intensity and deformation

	Max' Stress Intensity, SMX (KN/m ²)	Max' Deformation, DMX (mm)
2 Φ 5.6	189	6.56
2 Φ 4.0	184	2.94
2 Φ 2.8	183	2.94

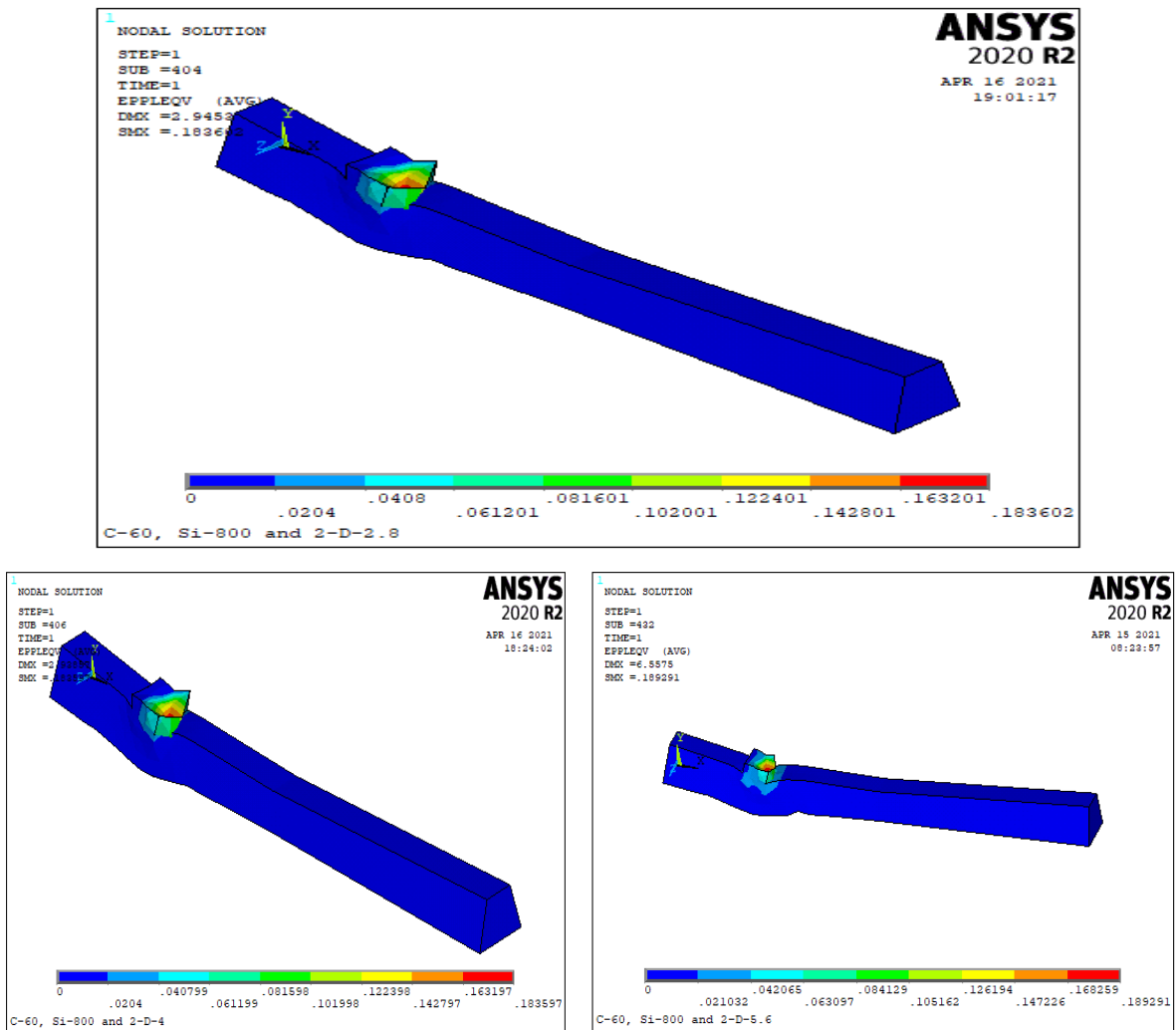


Figure 4. 10 Stress intensity and deformation graph for C-60 and 800MPa sleeper

Generally, as the diameter of steel bars decreases, the maximum stress intensity of the specimen and its maximum deformation decreases.

4.3.4 Effect of number of prestressing bars

The parametric investigation is conducted on three models to study the number of prestressing steel bars. Railway sleepers with 2Φ4, 3Φ4, and 4Φ4 tendons with C-60 concrete grade and 800MPa initial stress bars are used. The analysis results are discussed in the following subsection based on load-displacement responses, stress intensity, maximum deflection, and plastic strain from ANSYS 2020 R2 results.

I. Effect of the number of bars on load-displacement responses

The load-displacement response of specimens is presented in comparing their peak loads.

Table 4.9 Comparison on load capacity due to effect of the number of bars

	Load (peak), N	Displacement @ peak load, mm
2 Φ 4.0	60,611	0.323
3 Φ 4.0	60,733	0.323
4 Φ 4.0	60,752	0.314

As shown in the above table, sleepers with 2Φ4, 3Φ4, and 4Φ4 prestressing steel bars yields a peak load of 60,611N, 60,733N and 60,752N with corresponding deflections 0.323mm, 0.323mm and 0.314mm at yield load respectively. Generally, make other variables constant; as the number of bars increases, the maximum load-carrying capacity of the specimen is also increased, but the deflection at this load has decreased.

II. Effect of the number of bars on stress intensity and deformed shape response

From ANSYS non-linear analysis of the number of steel bars on railway sleepers, the average maximum stress intensity becomes 185KN/m² with a corresponding average maximum deflection of 2.94mm for 2Φ4, 3Φ4 and 4Φ4 prestressing steel bars, respectively.

Table 4.10 Effect of number of bars on maximum stress intensity and deformation

	Max' Stress Intensity, SMX (KN/m ²)	Max' Deformation, DMX (mm)
2 Φ 4.0	184	2.94
3 Φ 4.0	186	2.94
4 Φ 4.0	185	2.94

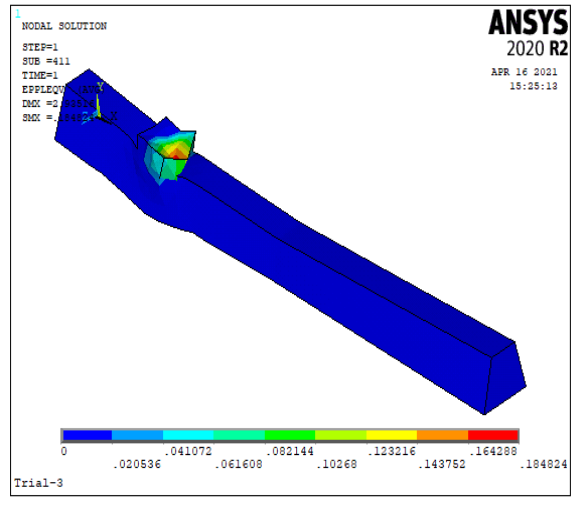
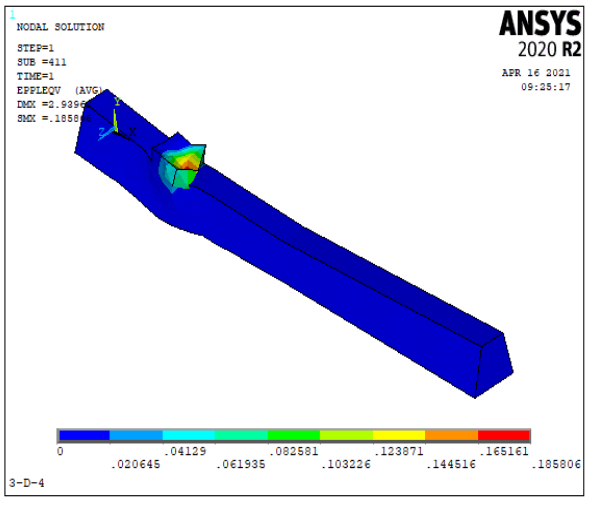
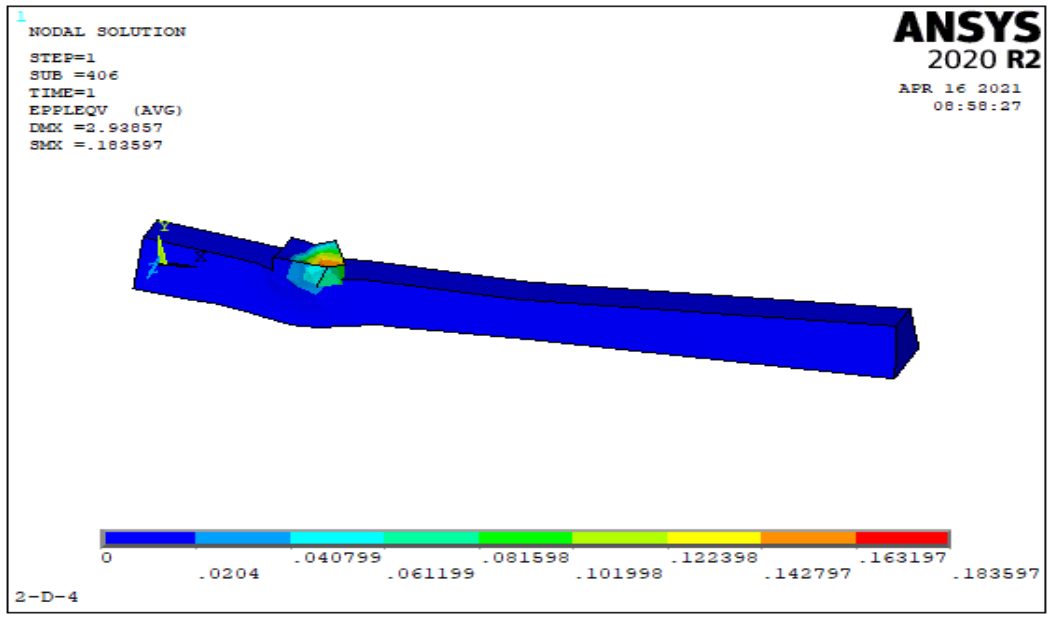


Figure 4. 11 Stress intensity and deformation graph for C-60, 800 MPa and $\Phi 4$ sleeper

Generally, as the number of steel bars varies, the specimen's maximum stress intensity and maximum deformation do not show any observable change. Therefore, the number of tendons has no considerable effect on sleepers' stress intensity and deformed shape response.

III. Effect of the number and diameter of bars on plastic strain response

The ANSYS analysis on railway sleepers made from C-40 grade of concrete results in a maximum plastic strain of $0.442E-5$, $0.416E-5$ and $0.285E-5$. Sleepers with $2\Phi 5.6$, $4\Phi 4$, and $8\Phi 2.8$ steel bars are initially stressed with 1200MPa are used (refer to figure 4.11).

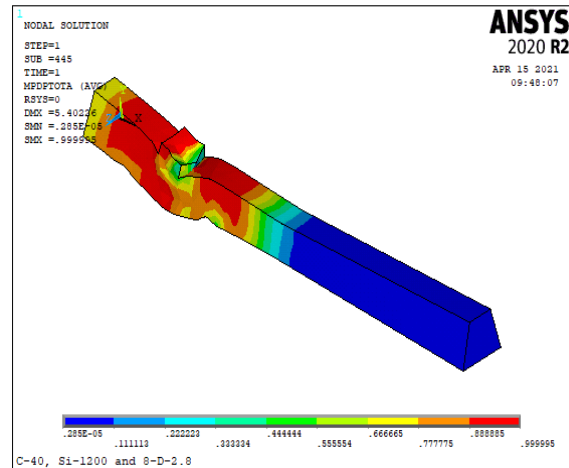
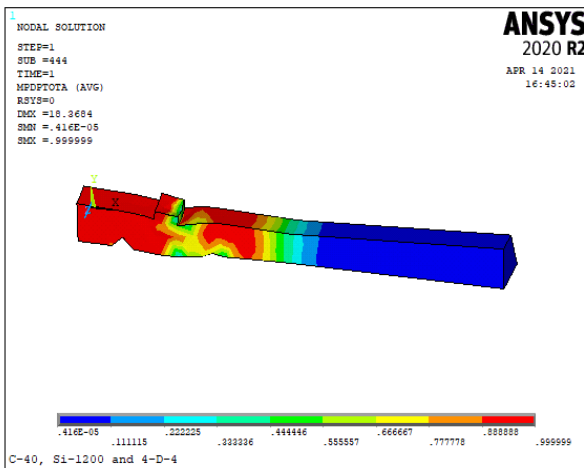
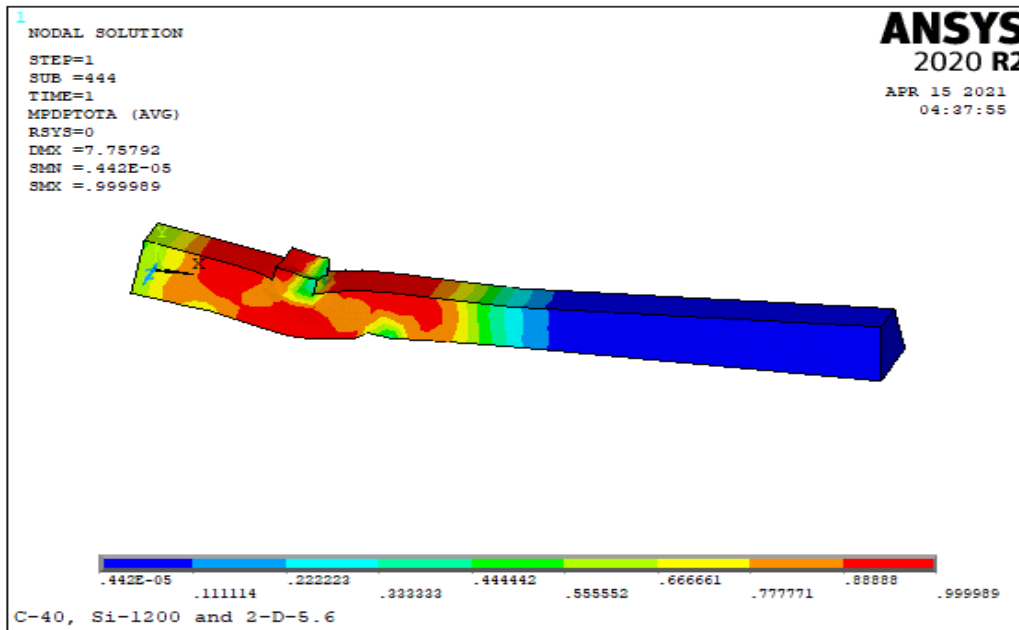


Figure 4. 12 Maximum plastic strain graph for C-40 and 1200 MPa sleeper

As the diameter of steel bars decreases from 5.6 to 4 and then to 2.8, the maximum plastic strain of the specimen shows a decrement to correspondingly for different initial stresses and grades of concrete of tendons. On the other hand, the specimen's ultimate plastic strain decreases while the number of bars increases.

4.3.5 Effect of position of prestressing bars

A parametric investigation is conducted on four models to study the impact of the position of tendons. Railway sleepers with C-60 grade of concrete and 800MPa stress initially applied to 2Φ5.6 steel bars are used. The equal number and size of bars are positioned at different locations to investigate bar position on prestressed concrete railway sleepers. The analysis results are discussed in the following subsection based on load-displacement responses, stress intensity, maximum deflection, and plastic strain from ANSYS 2020 R2 results.

I. Effect of the position of bars on load-displacement responses

The load-displacement response plots of C-60 grade concrete with 2Φ5.6 bars and 800MPa initial stress are presented compared to their peak loads, as shown in Table 4.11.

Table 4.11 Comparison on load-carrying capacity due to effect of position of bars

	Max' load, N	Displacement @max' load, mm
Bars @top	60,483	0.323
Bars @middle	60,637	0.311
Bars @bottom & top	60,692	0.323
Bars @bottom	60,861	0.323

As seen from the table, placing the bars at the bottom yields the highest load-carrying capacity and corresponding displacement than at the top and middle of the sleeper.

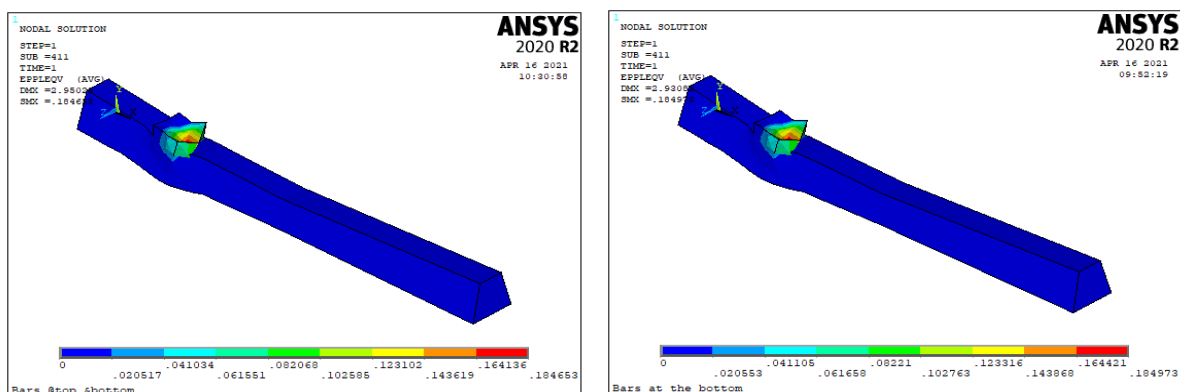
II. Effect of position of bars on stress intensity and deformed shape response

From ANSYS 2020 R2 analysis of C-60 grade of concrete and 800MPa initial stress on railway sleepers, the average maximum stress intensity becomes 182KN/m², 185KN/m², and 185 KN/m² with a corresponding average maximum deflection of 2.98mm, 2.95mm, and 2.93mm for bars positioned at the top, bottom & top and bottom of the sleeper respectively.

Table 4.12 Effect of position of bars on maximum stress intensity and deformation

	Max' Stress Intensity, SMX (KN/m2)	Max' Deformation, DMX (mm)
@top	182	2.98
@bottom & top	185	2.95
@bottom	185	2.93

As the position of steel bars is changed from the top to the bottom, the maximum stress intensity of the specimen is increased, whereas its maximum deformation shows some decrement.



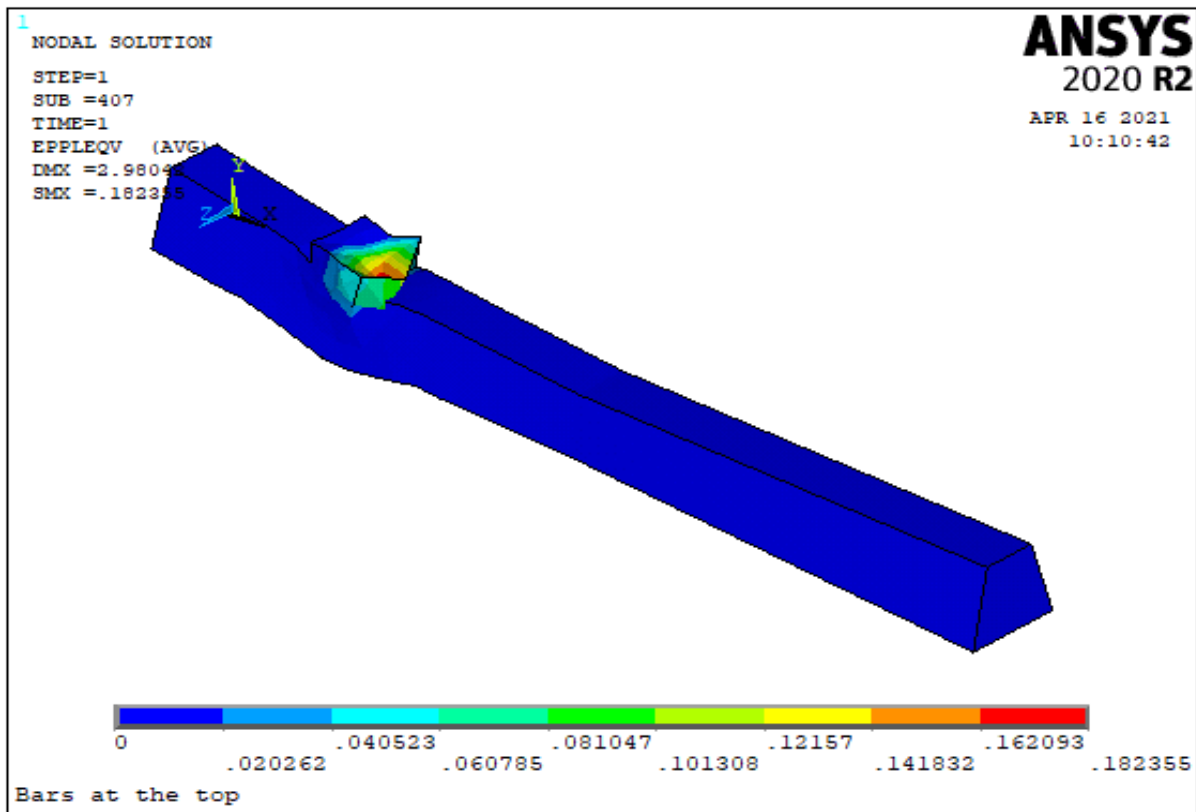


Figure 4. 13 Stress intensity and deformation graph for C-60, 800 MPa and 2Φ5.6 sleeper

4.3.6 Summary of results

The following table describes the summary of relations of variables with nonlinear FEA outputs for each specimen analyzed by the ANSYS Mechanical APDL 2020 R2 software package.

Table 4. 11 Summary of results

	Maximum Load	Displacement at max' Load	Maximum Stress Intensity	Maximum Deformation	Maximum Plastic Strain
Grade of Concrete	+	+	+	-	+
Initial Stress of Bars	0	0	0	0	0
Number of Bars	+	-	0	0	-
Diameter of Bars	+	-	+	+	+

Note: “+” indicates the variables have a positive or direct effect on the outputs.

“0” indicates the variables have no significant effect on the outputs.

“-” indicates the variables have a negative or inverse effect on the outputs.

CHAPTER FIVE

5 CONCLUSIONS AND RECOMMENDATIONS

5.1 Introduction

This thesis investigated the effect of prestressing steel bars on prestressed steel fibre reinforced concrete railway sleepers' behaviour. To examine the results of the number, position, diameter, initial stress of tendons, and the grade of concrete, on the load-displacement responses, maximum stresses, and plastic strain properties of sleepers under static loading, a wide-ranging parametric study has been carried out.

5.2 Conclusions

From the NLFEA results carried out in this study on the behaviour of steel fibre reinforced concrete railway sleepers under static loading, the following conclusions can be drawn:

- ✓ The NLFE modelling confirms the capability of the model to predict the behaviours of prestressed SFRC railway sleepers. The maximum load model prediction leads to about a deviation of 6.5% and 10%, respectively, with the experimental and analytical results.
- ✓ FEA results indicate an increase in the grade of concrete improved load carrying capacity of sleepers, about a 17.75 % average increment for each 10 MPa. Generally, for all specimens, as the grade of concrete increases load-carrying capacity of sleepers increases, and then the overall performance of sleepers is enhanced in terms of load-bearing capacity and deflection serviceability. Besides this, increasing the grade of concrete by 10MPa also increased the maximum stress intensity of the sleeper by 3.88%. In addition, it decreased its maximum deformation by 11.39%.
- ✓ Based on the ANSYS results, the initial stress of bars has no significant effect on the load-bearing capacity and maximum stress intensity. However, when their magnitude has increased, the ultimate plastic strain of bars shows a corresponding increment.
- ✓ According to the FEM analysis result, the number and diameter of prestressing bars positively affect the load-bearing capacity of the specimen. A 1.4mm average increase in the diameter of bars inhibits about a 0.3% rise in its load-carrying ability. When the diameter of steel bars has increased, the maximum plastic strain of bars has also increased. Still, the maximum stress intensity shows a 1.6% increment. Furthermore, the number of steel bars has no observable effect on the maximum stress intensity and maximum deformation of sleepers.

- ✓ The other thing noticed from this research is that positioning steel bars at the bottom rather than at the top and middle of the sleeper is preferred for the best capacity of railway sleepers. Moving tendons from top to middle and then the bottom of sleepers shows a 0.31% average increment in its load-carrying capacity.

5.3 Recommendations and Further studies

During this study, some research areas appeared to need further investigation on the behaviour of SFRC prestressed railway sleepers. Based on the work conducted in this research, the following can be recommended for future work:

- ✓ This study has been numerically investigated the effects of tendons on prestressed concrete railway sleepers' behaviour under static loading. The author of this research work recommends a large-scale experimental investigation of sleepers under impact loadings.
- ✓ This research is performed on Indian railway standards and Monoblock sleepers; other studies can be extended for different sleepers.
- ✓ The current nonlinear finite element models are developed using the perfect bond modelling approach. Further numerical models are called to predict the pinching behaviour of steel bar-concrete connections under impact loading. It may be by adopting bond-slip models, and employing the pinching of the hysteretic response is highly recommended.

REFERENCES

- A.R.Foan. (2011). Eighteen months service under 40 tone axle load. *Proceeding of excellence in heavy haul railroading*.
- Alex M. Remennikov and Sakdirat Kaewunruen. (2008). A review of loading conditions for railway track structures due to train and track vertical interaction. *Structural control and health monitoring*, 207-234.
- Amare, K. (2017). Design of Prestressed Concrete Sleeper Based on Ultimate Limit State. *AAiT, unpublished thesis*.
- Amlan K. S. and Devdas M. (2008). Prestressed Concrete Structures. *Indian Institute of Technology Madras, Online Version*.
- Anand Raj, P. N. (2018). A Review on the Development of New Materials for Construction of Prestressed Concrete Railway Sleepers. *Materials Science and Engineering*.
- Anand Raj, Praveen Nagarajan, and A P Shashikala. (2020). Investigations on Fiber-Reinforced Rubcrete for Railway. *ACI STRUCTURAL JOURNAL*.
- AREMA. (2014). American Railway Engineering and Maintenance-of-way Association. *American Railway Engineering and Maintenance-of-way Association*.
- AS1085.14. (2003). Australia standard, Railway track materials, Part 14. *Railway prestressed concrete sleepers*.
- C, E. (2001). Modern Railway Track. *The Netherlands MRT Press*.
- Chanh, N. V. (2015). Steel Fiber Reinforced Concrete. *The Ho Chi Minh City University of Technology, Faculty of Civil Engineering*, 108-116.
- Gebeyehu, Y. (2012). Standardization Of Guidelines For Railway Track. *Unpublished a thesis submitted to the school of Graduate Studies of Addis Ababa University*.
- Greve M J, Dersch M S, Edwards J R, Barkan C P, Mediavilla J, and Wilson B. (2016). Effect of particle intrusion on rail seat load distributions on heavy haul freight railroads. *International Journal of Rail Transportation* 4(2), 98-112.
- H.J.Taylor. (1993). The railway sleeper: 50 years of pretension, prestressed concrete. *Structural Engineer, Volume 71*.
- Jiang, H. & Zhao, J. (2015). Calibration of the continuous surface cap model for concrete. *Finite Elements in Analysis and Design*. 97, 1-19.
- J. Sýkorová, J. Bártová, P. Štemberk. (2012). Prestressed Concrete Sleeper Under Extreme Loading. *18th International Conference Engineering Mechanics*, 222.

- Kaewunruen, S. A. (2011). Experiments into Impact Behavior of Railway Prestressed. *Engineering Failure Analysis*, 2303-2315.
- Martin H. & B.Jian. (2012). The ultimate limit states the design of concrete railway sleepers. *Proceedings of the ICE - Transport*, 165 (3), 215-223.
- Parvez A and Foster S J. (2017). Fatigue of steel-fibre-reinforced concrete, prestressed railway sleepers. *Engineering Structures*, 241-250.
- Remennikov A M and Kaewunruen S. (2014). Experimental load rating of aged railway concrete sleepers. *Engineering Structures*, 147-62.
- Rezaie, F., Shiri, M. R., & and Farnam, S. M. (2012). Experimental and Numerical Studies of Crack Control for Prestressed Concrete sleepers. *Engineering Failure*, 21-30.
- Sadeghi J, Kian A R and Khabbazi A. (2016). Improvement of Mechanical Properties of Railway Track Concrete Sleepers Using Steel Fibers. *Journal of Materials in Civil Engineering*.
- Sakdirat Kaewunruen, Alexander Remennikov and Martin H. Murray. (2012). Limit states design of concrete railway sleepers. *Proceedings of the Institution of Civil Engineers: Transport*, 165 (TR2), 81-85.
- Sakdirat Kaewunruen and Alex M. Remennikov. (2015). Impact response of prestressing tendons in concrete railway sleepers in high-speed rail environments. *Computational Methods in Structural Dynamics and Earthquake Engineering*, 25-27
- Shayanfar, M. A., Kheyroddin, A. and Mirza, M. S. (1997) "Element size effects in the non linear analysis of reinforced concrete members," *Computers and Structures*, 62(2), pp. 339–352. DOI: 10.1016/S0045-7949(96)00007-7.
- Tlemat, H., Pilakoutas, K. and Neocleous, K. (2006) "Modelling of SFRC using inverse finite element analysis," *RILEM Materials and Structures*, 39(286), pp. 221–233.
- Toshan Rampat, Louis Le Pen, William Powrie, John Harkness. (2019). Evaluating the performance of different sleeper shapes and materials. *Faculty of Engineering and Physical Sciences, University of Southampton, United Kingdom*.
- Wit Derkowski, Bartłomiej Słyś, Maciej Szmit. (2014). Effect of strands' anchorage system in pc railway sleepers. *8th International Conference AMCM*.
- Zekeri and Sadeghi. (2007). investigation on the accuracy of current practice in the analysis of railway track sleepers. *International journal of civil engineering*, 34-51.
- Zreid, I. & Kaliske, M. (2018). A gradient enhanced plasticity-damage Microplane model for concrete. *Computational Mechanics*. 10(1007), 00466-018-1561-1.

APPENDICES

APPENDIX-A: SAMPLE MODELING OF SPECIMENS

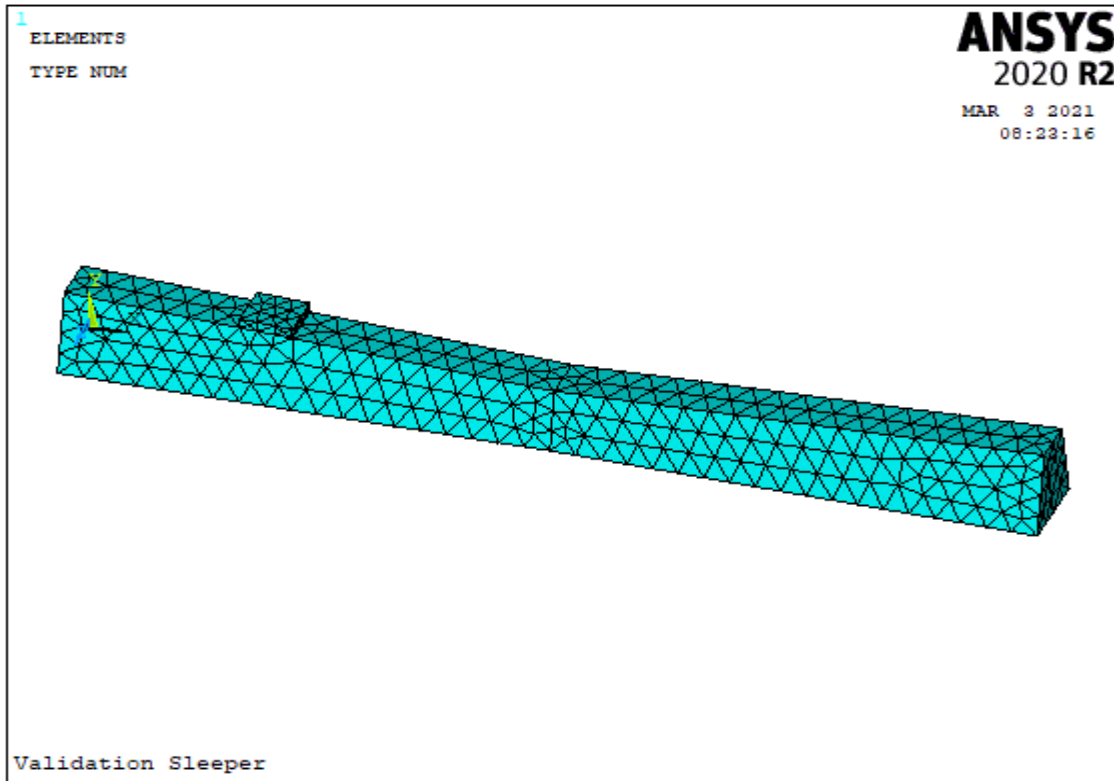


Figure A-1: Sample model element type and meshing (Validation Sleeper)

APPENDIX-B: ANSYS MECHANICAL APDL 2020 R2 INPUT FILES

Element and Material Property

/prep7

! Units: yield strength or pressure in MPa, Force in N and length in mm

! Element type

ET,1,215

keyopt,1,18,2 ! activates the 2 extra DOFs

ET,100,185

! SFRC material property definition

fcm= 74 ! SFRC mean characteristics strength

fuc = fcm*0.85 ! SFRC cylinder strength

nu = .2

E = 40100

fub = 1.15*fuc

fut = 1.4*(fuc/10)**(2/3)

Rt = 1

Dx = 4000

sigVc0 = -1.3*fuc

R=2

c = 1600

m = 2.5

gamt0 = 0

gamc0 = 2e-5

betat = 3000

betac = 2000

MP, EX,1, E

MP, NUXY,1, nu

TB, MPLA, 1,,DPC


```

TBDATA,1, fuc, fub, fut, Rt, Dx, sigVc0
TBDATA,7, R, gamt0, gamc0, betat, betac
TB, MPLA, 1,,NLOCAL
TBDATA,1, c, m
! Material reference number 2
MP, EX,2,200000      ! Main steel rebar modulus of elasticity
MP, NUXY,2,0.3      ! Main steel rebar Poisson ratio
TB, BISO,2
TBDATA,1,1715,1000  ! 1715 MPa Main steel rebar Yield strength
MP, EX,3,200000      ! steel plate for loading
MP, NUXY,3,0.3      ! steel plate Poisson ratio

```

Initial Stress

```

/prep7
! select elements with material number 2
ALLSEL, ALL
ESEL, ALL
ESEL, S, MAT,2
! select elements with material number 2 and apply initial stress 800 MPa
inistate, set, mat,2
inistate, set, dtyp, stre
inistate, define, ALL,,800
ALLSEL, ALL      ! select all

```

Create Concrete and Mesh

```

/prep7
      ! create concrete
K,1,0,0,0,
K,2,0,60,12.5,
K,3,0,60,62.5,

```

K,4,0,0,75,
K,5,925,0,0,
K,6,925,60,12.5,
K,7,925,60,62.5,
K,8,925,0,75,
LSTR, 1, 2
LSTR, 2, 3
LSTR, 3, 4
LSTR, 4, 1
LSTR, 5, 6
LSTR, 6, 7
LSTR, 7, 8
LSTR, 8, 5
LSTR, 1, 5
LSTR, 2, 6
LSTR, 3, 7
LSTR, 4, 8
FLST,2,4,4
FITEM,2,3
FITEM,2,2
FITEM,2,1
FITEM,2,4
AL, P51X
FLST,2,4,4
FITEM,2,5
FITEM,2,8
FITEM,2,6
FITEM,2,7
AL, P51X

FLST,2,4,4
FITEM,2,9
FITEM,2,10
FITEM,2,5
FITEM,2,1
AL, P51X
FLST,2,4,4
FITEM,2,11
FITEM,2,10
FITEM,2,2
FITEM,2,6
AL, P51X
FLST,2,4,4
FITEM,2,12
FITEM,2,9
FITEM,2,4
FITEM,2,8
AL, P51X
FLST,2,4,4
FITEM,2,3
FITEM,2,7
FITEM,2,11
FITEM,2,12
AL,P51X
FLST,2,6,5,ORDE,2
FITEM,2,1
FITEM,2,-6
VA,P51X
FLST,2,6,5,ORDE,2

```
FITEM,2,1
FITEM,2,-6
VA,P51X
      ! loading plate      ! # volume 3
BLOCK,165,215,60,70,12.5,62.5,
!ADD
FLST,2,2,6,ORDE,2
FITEM,2,2
FITEM,2,-3
VADD,P51X
      ! mesh areas
LSEL,All
Lsize,all,e1
! line element size
*SET,e1,25 ! element size 'e1'
LSEL,All
Lsize,all,e1
      ! Mesh concrete
ALLSEL,ALL
TYPE,100
MSHKEY,0
MSHAPE,1,3d
CHKMSH,'VOLU'
VMESH,ALL
VSEL,ALL
VSEL,S,LOC,Y,60,70
VSEL,A,LOC,Y,60,70
ESLV,R
MPCHG,2,ALL
```

!merges all simmilar nodes and elements

esel,all

NSEL,ALL

NUMMRG,NODE, , , ,LOW

NUMMRG,KP, , , ,LOW

Create Steel Rebars and Mesh

/prep7

NUMCMP,LINE ! compress line number

NUMCMP,AREA ! compress area number

! Longitudinal rebar section definition

SECTYPE,1,REINF,DISC ! Section reference#1

SECDATA,2,12.566,mesh ! Section data; material 2, 4 mm rebar with x-sectional area of
! 12.566 mmm2

!Main rebar

! creat one line element and copy paste into four location to get

! four main rebars parallel to X - axis

! concrete cover 20mm

k,4001,20,15,22.5 ! creat key point 4000

k,4002,905,15,22.5 ! creat key point 4001

l,4001,4002 ! creat line using above keypoints to generate one main rebar

*GET, nn1, LINE, 0, NUM, MAX, , ! assign nn1 = above created line number

LSEL,S, , , nn1 ! selected line numner nn1

LGEN,2,all, , , , 30 , , , 0 ! copy paste line number nn1 to generate additional main rebars

LSEL,S, , , nn1 ! selected line numner nn1

LGEN,2,all, , , , 30 , , , 0 ! copy paste line number nn1 to generate additional main rebars

*GET, nn2, LINE, 0, NUM, MAX, , ! assign nn1 = above created line number

! Mesh main rebar

et,200,200,2 ! mesh200 place holder

! Mesh

```

TYPE, 200
MAT, 2
REAL,
ESYS, 0
SECNUM, 1
LSEL,S,,nn1,nn2
lesize,all,,1
LSEL,S,,nn1,nn2
lmesh,all
/eshape,1
esel,all
nset,all
EREINF
! creat reinf264 elements; this are steel rebar elements automatically generated from
! placeholder mesh200 elements from base element 185
/eshape,1
esel,all
nset,all
EREINF
esel,all
NSEL,ALL

```

Loading and Boundary Conditions

```

/Solution
! Loading
NSEL,S,LOC,Y, 70
D,All,UY,- 5 ! displacement controlled loading; 5mm in negative Y-direction
! Pin boundary condition @ X=95
NSEL,S,LOC,X,100
NSEL,R,LOC,Y,0

```

D,All,UX,0

D,All,UY,0

D,All,UZ,0

! Pin boundary condition @ X=285

NSEL,S,LOC,X,275

NSEL,R,LOC,Y,0

D,All,UX,0

D,All,UY,0

D,All,UZ,0

esel,all

nset,all

! load substeps

TIME,1

NSUBST,50, 1000, 15, on ! starting substep=50, maximum substep=1000,

! minimum substep=15, automatic time stepping is on

OUTRES,ALL,1 ! WRITE ALL OUTPUT

SOLVE

SAVE

FINISH

Load Deflection Plots

finish

/prep7

! loading nodes

NSEL,S,LOC,Y, 70

*GET, n_min, NODE, 0, NUM, MIN, ,

*GET, n_max, NODE, 0, NUM, MAX, ,

*GET, n_count, NODE, 0, COUNT, , ,

finish

/POST1

```

SET, LAST
finish
/POST26
ii=n_min
*do,i,1,n_count-1,1
rforce,2,ii,F,y,FY
ADD,3,3,2,,FYT,,,-0.001, ! 0.001 is to change force N into KN out put
ii=NDNEXT(ii)
*ENDDO
n_uy=NODE(190,70,37.5) ! node coordinate at which deflection is read, here Uy
deflection or set n_uy = node number
NSOL,4,n_uy,U,Y,UY
ABS,4,4,,UY
/AXlab,X,displacement [mm]
/AXlab,Y,force [kN]
XVAR,4
PLVAR,3

```

Concrete Damage Plots

```

/POST1
esel,s,Mat,,1 ! select concrete material
/trlcy,elem,0
SET, LAST
plnsol,eppl,eqv ! plot major cracks, equivalent plastic strain
/wait,1 ! wait 1 second
plnsol,mpdp,tota ! plot minor cracks
/wait,1 ! wait 1 second
esel, s,type,,201
plnsol, eppl, eqv ! plot steel rebars equivalent plastic strain
/wait,1

```